UPPSALA
UNIVERSITET

UPTEC X 21043
Examensarbete 30 hp
December 2021

The use of a CRISPR-Cas9 system to protect probiotic strains from transferrable drug resistance genes

Sara Lundberg

UPPSALA
UNIVERSITET

Teknisk- naturvetenskaplig fakultet
UTH-enheten

Besöksadress:
Ångströmlaboratoriet
Lägerhyddsvägen 1
Hus 4, Plan 0

Postadress:
Box 536
751 21 Uppsala

Telefon:
018 – 471 30 03

Telefax:
018 – 471 30 00

Hemsida:
http://www.teknat.uu.se/student

Abstract

The use of a CRISPR-Cas9 system to protect probiotic strains from transferrable drug resistance genes

Sara Lundberg

The discovery of antibiotics have revolutionized modern medicine, facilitating the treatment of a variety of bacterial infections, enabled surgeries otherwise impossible to perform and increased life expectancy in all countries. However, the rapid development of resistance among microorganisms and the increasing numbers of clinical outbreaks caused by multiresistant bacteria have accelerated the need for new alternatives to antibiotics. Probiotic bacteria armed with defense systems have been studied as potential substitutes of antibiotics. These probiotic competitors can still contribute to the spread of resistance genes among microorganisms through horizontal gene transfer.

The aim of this study was to investigate whether constructed CRISPR-Cas9 systems have the potential to protect probiotic bacteria against horizontal transfer of antibiotic resistance genes. Transformation, transduction and conjugation assays in strains carrying or not carrying a plasmid-bourne CRISPR-Cas9 system were performed in order to compare the frequencies of transfer of the most common resistance genes.

The transformation and transduction assays demonstrated that the constructed CRISPR-Cas9 system entails a decrease in efficiency of transfer for targeted resistance genes. Moreover, it can be concluded that potentially increasing Cas9 levels by reducing its degradation results in increased prevention of horizontal gene transfer through transformation and transduction. Finally, we state that the CRISPR-Cas9 system does not result in protection against antibiotic resistance genes entering the cells through conjugation.

Handledare: Sanna Koskiniemi
Ämnesgranskare: Linus Sandegren
Examinator: Peter Kasson
ISSN: 1401-2138, UPTEC X 21043

Populärvetenskaplig sammanfattning

Antibiotika har sedan upptäckten för mer än 100 år sedan revolutionerat modern sjukvård och används runt om i världen för att behandla infektioner orsakade av bakterier. Ett stort hot som av många benämns som den tysta epidemin, uppstår när mikroorganismer utvecklar ett motstånd mot antibiotika. Mikrobiell resistens mot antibiotika kan uppkomma spontant genom att den genetiska informationen slumpmässigt förändras när mikroorganismerna förökar sig. Resistensen kan, förutom att uppstå på grund av slumpmässiga förändringar även spridas mellan olika mikroorganismer när dessa tar upp fri arvsmassa eller kommer i kontakt med andra mikroorganismer eller virus som överför genetiskt material.

Varje år dör flera hundra tusen människor efter att ha infekterats av antibiotikaresistenta bakterier. Den utbredda överanvändningen av antibiotika har bidragit till att spridningen av resistens mellan olika mikroorganismer har ökat explosionsartat och antalet människor som mister livet när inga tillgängliga antibiotika kan användas för behandling av dessa organismer förväntas fortsätta stiga snabbt de kommande tiotal åren. Av denna anledning behöver nya alternativ till antibiotika utvecklas för att undvika en medicinsk katastrof.

Ett potentiellt exempel på alternativ till antibiotika är att använda sig av goda bakterier (probiotika) som "slåss" mot bakterier som orsakar farliga infektioner. Dessa bakterier har naturliga eller syntetiskt konstruerade försvarssystem som sänder ut gifter för att bekämpa motståndare. Men dessa probiotiska bakterier kommer ständigt att komma i nära kontakt med andra arter och virus och kan därför komma att bidra till spridningen av resistens.

Emmanuelle Charpentier och Jennifer Doudna tilldelades Nobelpriset i kemi år 2020 för deras upptäckt av CRISPR-Cas9 systemet även kallad gensaxen. Systemet som naturligt används av bakterier som ett försvar mot virusinfektioner, utvecklades av nobelpristagarna som ett dynamiskt verktyg för att förändra arvsmassan i olika typer av celler. Gensaxen har stor medicinsk potential och hoppas i framtiden kunna användas i behandling av till exempel cancer och autoimmuna sjukdomar.

I detta projekt kommer gensaxens potential att förhindra upptag av antibiotikaresistens att undersökas genom att analysera hur stor andel av bakterierna (med eller utan gensax) som utvecklar resistens. Om färre bakterier med gensax utvecklar resistens mot antibiotika innebär det att man kan använda detta system för att förhindra probiotiska bakterier från att sprida resistens.

Table of contents

1 Abbreviations

CDI	Contact-dependent growth inhibition
CRISPR	Clustered Regularly Interspaced Short Palindromic Repeats
crRNA	CRISPR RNA
ESBL	Extended spectrum β-lactamase
DHFR	Dihydrofolate reductase
DHPS	Dihydropteroate synthase
DNA	Deoxyribonucleic acid
HGT	Horizontal Gene Transfer
LA	Luria–Bertani Agar
LB	Lysogeny Broth
MIC	Minimal inhibitory concentration
oriT	Origin of transfer
PABA	Para-aminobenzoic acid
PAM	Protospacer adjacent motif
PBP	Penicillin-binding protein
PCR	Polymerase Chain Reaction
RCR	Rolling circle replication
RNA	Ribonucleic acid
RpoB	RNA polymerase B
T4SS	Type IV secretion system
UTI	Urinary tract infection
WHO	World Health Organization

2 Introduction

2.1 Antibiotics

Antibiotics are naturally produced compounds or partially synthetic derivatives of such that limit bacterial growth through a variety of mechanisms (Lerminiaux *et al.* 2019). The first clinical antibiotics, sulfonamides, are commonly overshadowed by penicillin that received considerable publicity after the discovery in 1928 (Hutchings *et al.* 2019). The subsequent revolution of medicine resulting from the introduction of antibiotics has facilitated the treatment of bacterial infections and increased life expectancy in all countries (Singh *et al.* 2017). In addition, antibiotics have further contributed to medicine by allowing surgeries such as transplantation of organs and cancer treatments otherwise not possible to perform.

Some antibiotics have a broad-spectrum and can actively target both Gram-positive and Gram-negative bacteria, whereas others have a more narrow spectrum of activity, targeting only a small number of bacteria (Singh *et al.* 2017). Derivatives of naturally produced antibiotics have been chemically modified in a series of steps based on structural studies to generate improved agents with higher efficiency (Singh *et al.* 2017). Clinical antibiotics have been structured into major classes that include β-lactams, macrolides, aminoglycosides, tetracyclines, quinolones and sulfonamides (Singh *et al.* 2017).

2.1.1 β-lactam antibiotics inhibits the cell wall synthesis

The β-lactams are the most prevalently prescribed class of antibiotics and the mechanism of action was initially described by Tipper and Stominger (1965) (Tooke *et al.* 2019). The β-lactams show a broad spectrum of activity and high antimicrobial efficiency (Singh *et al.* 2017). The chemical modification of penicillin, cephalosporin and carbapenem side groups have resulted in around 100 semi-synthetic derivative agents in the course of 75 years (Singh *et al.* 2017).

All β-lactams possess a characteristic β-lactam ring and interfere with the synthesis of the cell- wall by multi-target binding to penicillin-binding proteins (PBPs) (Singh *et al.* 2017). PBPs are enzymes that synthesise and construct the peptidoglycan in the cell-wall (Singh *et al.* 2017). In the presence of the antibiotic, PBPs cause a nucleophilic reaction with the β-lactam ring resulting in acetylation of PBPs and thereby inactivation of cell wall synthesis (Tooke *et al.* 2019). β-lactams are further divided into penicillins, cephalosporins, carbapenems and monobactams based on the architecture of the varying second fusion ring (Singh *et al.* 2017). Penicillins, cephalosporins and carbapenems

carry a thiazolidine, dihydrothiazine and pyrroline ring respectively whereas monobactams lack a second ring (Tooke *et al.* 2019).

2.1.2 Macrolides targets the 50S RNA of the bacterial ribosomes

Macrolides are commonly used to treat respiratory infections and have been in clinical practise for over 50 years (Singh *et al.* 2017). The antibiotics are characterised by their macrolactone rings and have variable side chains (Lenz *et al.* 2021). Protein synthesis is interfered by macrolides through binding to the 23S rRNA in the 50S ribosomal subunit (Singh *et al.* 2017). Structural research has demonstrated that the macrolactone ring binds to the nascent peptide exit tunnel and thereby disturbs the extension of polypeptide chains (Lenz *et al.* 2021). Studies have shown however, that the mode of action is more complex as the translation of specific polypeptides is not inhibited (Starosta *et al.* 2010). The details behind the exact binding and selection of proteins in this proposed model have not been clarified. The ribosomal target of macrolides is conserved in both Gram-positive and Gram-negative species, however the structure of the outer membrane in most Gram-negative bacteria prevents macrolides from reaching the ribosomal target (Myers & Clark 2021).

The first macrolide to be identified, erythromycin has a broad spectrum of activity and is reported as one of the most frequently prescribed macrolides (Lenz *et al.* 2021). Treatment with macrolide antibiotics confer low toxicity and a low occurrence of allergic issues (Lenz *et al.* 2021). Resistance against macrolides, such as erythromycin, in *Streptococcus pneumoniae* has restricted the clinical use of macrolides to treat respiratory tract infections (UTIs) (Singh *et al.* 2017).

2.1.3 Aminoglycosides target the ribosomal 30S subunit

Aminoglycosides carry a characteristic derivative of inositol coupled to a minimum of one sugar where the hydroxyl group is replaced with an amine group (Becker & Cooper 2013). They bind the ribosomal 30S subunit and interfere with protein synthesis (Singh *et al.* 2017). The binding occurs through the interaction of free hydroxyl and amino groups in the aminoglycoside and the 16S rRNA of the smaller subunit (Becker & Cooper 2013).

The first aminoglycoside to be discovered, streptomycin, was also the first antibiotic to cure patients from tuberculosis (Becker & Cooper 2013). Clinical use of aminoglycosides has decreased due to experienced ototoxicity (ear damage) and nephrotoxicity (kidney damage) from patients treated with aminoglycosides as well as the development of resistant bacteria (Singh *et al.* 2017). The more extensive development in other

wide-spectrum antibiotics classes such β-lactams and fluoroquinolones presenting less side effects have decelerated the search for new aminoglycosides and arbekacin was the last aminoglycoside to reach the market in 1990 (Becker & Cooper 2013; Correia *et al.* 2017).

2.1.4 Tetracyclines target the 30S RNA of the bacterial ribosome

Tetracyclines are broad-spectrum antibiotics that have been in clinical use for over 60 years (Singh *et al.* 2017). 37 % of the antimicrobial compounds used for livestock in the European Union consist of tetracyclines (Møller *et al.* 2016). Treatments with tetracyclines have low occurrence of reported side effects and are used preventively against the spread of malaria originating from *Plasmodium falciparum* (Chopra & Roberts 2001). In addition, tetracyclines are used as feed supplements in order to promote growth in animals (Chopra & Roberts 2001). The extensive use of tetracyclines has led to a rapid selection of resistant microorganisms (Chopra & Roberts 2001).

The core structure of tetracycline antibiotics, four cyclic rings, is accompanied by varying side groups (Chopra & Roberts 2001). Tetracyclines bind to the 16S rRNA in the 30S subunit of bacterial ribosomes and thereby disturb translation by blocking the coupling of aminoacyl-tRNA to the ribosomal acceptor (A) site (Muthukrishnan *et al.* 2012).

2.1.5 Quinolones interfere with DNA synthesis

The core of quinolone antibiotics is a bicyclic structure that is accompanied by five varying side chains (Pham *et al.* 2019). The synthetic quinolones have been used as antimicrobial agents for around 35 years and prevent DNA synthesis by interfering with DNA gyrase and topoisomerase IV (Singh *et al.* 2017). DNA gyrase and topoisomerase IV acts as catalysts in the supercoiling of DNA (Correia *et al.* 2017).

The first generation of quinolones were used predominantly to treat infections caused by Gram-negative pathogens (Correia *et al.* 2017). The second generation of quinolones, fluoroquinolones, have successfully enhanced the antimicrobial efficiency and broadened the activity spectrum to include Gram-positive pathogens in addition to additional Gram-negative pathogens (Singh *et al.* 2017). The fluoroquinolone ciprofloxacin, discovered in the 1980s, is still one of the most frequently prescribed antibiotics and has been named as an essential medicine by the World Health Organization (WHO) (https://list.essentialmeds.org/) (Correia *et al.* 2017). The increased safety, bioavailability and improved pharmacokinetics of fluoroquinolones have resulted in an extensive use in applications such as treatment of UTIs and respiratory infections (Correia *et al.* 2017).

2.1.6 Sulfonamides interfere with the synthesis of folic acid

Antimicrobial sulfonamides are synthetic antibiotics that prevent the production of folic acid, which is a crucial growth factor (Scholar 2007). They share structural analogy with the folate synthesis intermediate para-aminobenzoic acid (PABA) (Scholar 2007). The core structure of antimicrobial sulfonamides contains an aromatic amine group as well as a sulfonamide group with variable side chains (Farah *et al.* 2018). As human cells receive folic acid solely from intake of food using a completely different transportation system, the sulfonamides are selectively targeting prokaryotic cells (Scholar 2007).

The activity spectrum includes Gram-positive as well as some Gram-negative pathogens including *Escherichia coli, Salmonella* and *Klebsiella* strains (Tacic *et al.* 2017). The broad spectrum of activity has been narrowed down due to the spread of sulfonamide resistance (Scholar 2007).

By themselves, they are used for treatment of UTIs, but in combination with other antibiotics such as trimethoprim, they are commonly used to treat other types of infections (Scholar 2007). The combination of the sulfonamide sulfamethoxazole and trimethoprim (co-trimoxazole) has been listed as an essential medicine by WHO (https://list.essentialmeds.org/). Co-trimoxazole is the most commonly used combination of trimethoprim and sulfonamides (Kalkut 1998). Trimethoprim binds to dihydrofolate reductase in bacteria and inhibits the formation of folic acid (Kalkut 1998).

2.2 The spread of antibiotic resistance is accelerated by horizontal gene transfer

The spread of antibiotic resistance between microorganisms is a growing issue worldwide and the number of bacteria carrying antibiotic resistance genes needs to decrease in order to reduce the risk of infections caused by multiresistant bacteria. Due to the intense use of antibiotics, the selection of bacteria with resistance genes towards most antibiotics used in medicine today is growing rapidly (Liu *et al.* 2016). The use of antibiotics contributes to the elimination of antibiotic-sensitive microorganisms and consequently results in a competitive advantage for bacteria carrying resistance genes (Lerminiaux *et al.* 2019). Without effective antibiotics, conditions such as urinary and respiratory tract infections can be life-threatening and an estimated 700 000 people each year die from diseases caused by resistant bacteria (WHO 2019). The number of deaths each year due to antibiotics resistance related diseases is expected to increase and has been predicted to reach 10 million by the year of 2050 (de Kraker *et al.* 2016).

The origin of antibiotic resistance includes a variety of mechanisms such as, upregulation of efflux pumps that evict the compounds from the cell membrane, chemical inactivation of the antibiotic or physical obstruction of the cell wall through alteration of metabolic pathways (Zinner 2007). The exchange of genetic material between microorganisms entails proliferation of antibiotic resistance. Antibiotic resistance can be developed by bacteria through spontaneous mutations (Zinner 2007), but to cause a pandemic as the one we are living in, the resistance genes have to be spread between bacteria. The resistance is primarily spread through horizontal gene transfer (HGT) (Bello-López *et al.* 2019). In the mechanism of HGT, foreign genetic material is spread between different microorganisms through conjugation, transformation and transduction (Tumuluri *et al.* 2021). An overview of the different mechanisms of HGT is presented in Figure 1

2.2.1 Conjugation is mediated by type IV secretion systems

In the process of conjugation, donor bacteria transfer DNA to recipient cells in a contact-dependent mechanism. Proteins from the type IV secretion system (T4SS) family as well as proteins with high similarities to bacterial rolling-circle replication (RCR) systems are involved in the conjugation mechanism (Llosa *et al.* 2002). The T4SS consists of four core parts, the pilus, the channel complex, the platform structure and the ATPases that contribute with transportation and pilus generation energy (Cabezón *et al.* 2015). Moreover, the conjugative system contains an additional protein considered as the coupling protein, that connects the RCR system to the secretion system (Llosa *et al.* 2002). Initially, the RCR-like complex binds to the origin of transfer (oriT) and creates a nick in the transferrable DNA strand and unwinds it (Llosa *et al.* 2002). The remaining strand is subsequently replicated and religated (Llosa *et al.* 2002). To transfer the DNA to the recipient cell, the coupling protein escorts the single stranded transferrable DNA to the T4SS (Llosa *et al.* 2002). The exact details of how the specific secretion process functions have not been clarified but different models have been proposed, such as the molecular motor model of the coupling protein by Llosa *et al.* (2002). In this model the coupling protein does not only guide the DNA to the T4SS, but actively pumps the DNA to the recipient cell.

2.2.2 Transformation mechanism requires specific conditions for competence

In contrast to conjugation, the mechanisms of gene transfer by transformation are controlled by the recipient bacteria and not the donor (Johnston *et al.* 2014). The competence to take up the DNA rely on the expression of a collection of conserved genes (Johnston *et al.* 2014). Multiple types of transformation models have been characterised for different strains of bacteria. The first strains to have their transformation mechanism

partially characterised were *Bacillus subtilis* and *Streptococcus pneumoniae* (Johnston *et al.* 2014). In these strains, double-stranded DNA is converted to single-stranded and the strand is transported into the recipient cell through a membrane channel (Johnston *et al.* 2014).

For the majority of bacteria, specific conditions are required to allow the uptake of foreign DNA into the bacterial cytosol (Johnston *et al.* 2014). These conditions can be induced by chemical transformation, electro-transformation and sonic transformation (Yoshida & Sato 2009). Chung *et al.* (1987) developed a streamlined transformation process with a transformation and storage solution (TSS) in order to prepare competent *E. coli*.

2.2.3 Bacteriophages transfer bacterial genetic material in the mechanism of transduction

Bacteriophages are viruses that bind to the cell membrane of bacteria and inject their DNA (Griffiths *et al.* 2000). In this way, phage genes can be expressed and new bacteriophages can be produced directly inside the host cell. The mechanism of transduction is divided into classes; general transduction or specific transduction (Griffiths *et al.* 2000). In the mechanism of general transduction, bacteriophages transfer variable parts of the whole donor chromosome whereas in specific transduction, bacteriophages transfer restricted sections of the chromosome (Griffiths *et al.* 2000).

The bacteriophage P1 was initially found in *E. coli* and is a generalized bacteriophage (Riquelme *et al.* 2019). P1 phages are capable of transducing plasmids as well as chromosomal genetic material of sizes up to 100 kb (Riquelme *et al.* 2019). The chromosome in the infected cells is fragmented and the fragments can accidentally be included in newly produced phage particles (Griffiths *et al.* 2000). In this way, bacteriophages can transfer genetic material to new cells after the lysis of the donor cell (Griffiths *et al.* 2000). The insertion of phage DNA in the new cells means that the bacterial genes can be incorporated into the recipients through recombination (Griffiths *et al.* 2000).

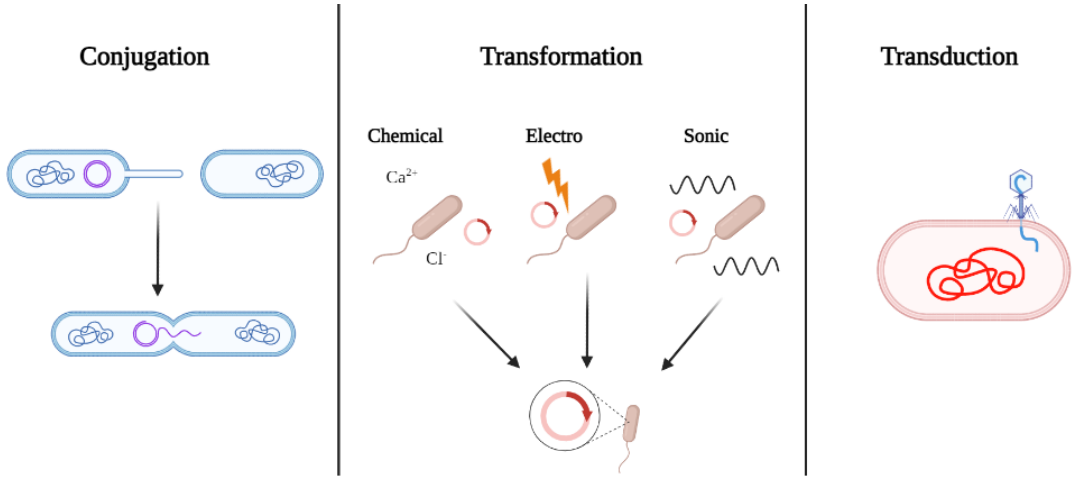

Figure 1: The figure presents an overview of the mechanisms of horizontal gene transfer; conjugation, transformation and transduction. Created with BioRender.com

2.3 Outbreaks of multiresistance plasmids cause great concern

The prevalence of multiresistant plasmids have increased over the years due to the large-scale practise of broad-spectrum antibiotics (Ogbolu *et al.* 2018). When spread through HGT, these multiresistant plasmids can cause clinical outbreaks where the infectious bacteria are resistant against a majority of the currently available antibiotics. Sandegren *et al.* (2012) determined the genomic sequence of a plasmid previously isolated from an outbreak of *K. pneumoniae* at the Uppsala University Hospital in 2005. The pUUH239.2 plasmid is a multiresistance plasmid with resistance genes; *oxa-1*, *ctx-m-15* and *tem-1* (beta-lactams), *aac-(6')-1b-cr* and *aadA2* (aminoglycosides), *tetA* and *tetR* (tetracyclines), *dhfrXII* (trimethoprim), *sul1* (sulphonamides) and *mph(A)-mrx-mphR(A)* (macrolides). *qacEΔ1* (quaternary ammonium compounds) and silver, copper and arsenic (heavy metal ions) genes are also contained on the plasmid. The *K. pneumoniae* strain carrying the pUUH239.2 plasmid infected 248 patients of which the majority were old or had compromised immune systems. The resistance genes on the pUUH239.2 plasmid target different antibiotics through a variety of mechanisms.

2.3.1 β-lactamases hydrolyse β-lactam antibiotics

The *ctx-m-15* (Cefotaximase-Munich-15) gene encodes an extended spectrum β-lactamase (ESBL) which in Gram-negative bacteria entails resistance against multiple β-lactam antibiotics such as penicillins and cephalosporins (Ogbolu *et al.* 2018). The penicillins and cephalosporins, such as cefotaxime, are hydrolysed by ESBLs and are

prevented from entering the periplasm (Ogbolu *et al.* 2018). Among ESBL expressing pathogenic *E. coli* strains in humans, the CTX-M-15 enzyme is the most commonly found in clinical isolates (Irrgang *et al.* 2017). Mutations in the active site of narrow-spectrum enzymes, causing a broader hydrolysis spectrum are commonly the cause of the emergence of ESBL (Paterson & Bonomo 2005). The *ctx-m-15* gene is originally derived from a chromosomal version of the gene in a *Kluyvera* species (Dedeic-Ljubovic *et al.* 2010).

The OXA-1 enzyme primarily confers resistance against isoxazolyl penicillins, such as oxacillin (June *et al.* 2014). The *bla*OXA-1 gene has been identified in clinical isolates of Gram-negative bacteria together with ESBL encoded genes and is commonly located in intergrons (Hussein *et al.* 2009; Poirel *et al.* 2002). The location in mobile elements and the rapid spread of *bla*OXA-1 cause concern in clinical contexts when certain antibiotics can not be used to treat infections (Bethel *et al.* 2008). Human isolates of *E. coli* with *bla*OXA-1 often aquire CTX-M-15, which results in resistance against also combinations therapies with β-lactam and β-lactamase inhibitors, that can overcome *bla*OXA-1 mediated β-lactam resistance, but not that of CTX-M-15 (Livermore *et al.* 2019).

ESBL genes are primarily accommodated on plasmids, making them highly susceptible for HGT (Isgren *et al.* 2019). *E. coli* and *Klebsiella* are the primary species carrying ESBL genes and plasmid-bourne ESBL genes are often joined by other β-lactamase genes and genes from different resistance families, resulting in multiresistance plasmids (Ogbolu *et al.* 2018). The limitations of therapeutic opportunities when it comes to treating pathogens carrying these multiple resistance genes cause great concern due to rapid spread of ESBL genes and the increased risk of mortality that comes with it (Ogbolu *et al.* 2018). Treatment options of ESBL-producing strains are sometimes limited to a combination of pharmaceuticals including β-lactamase inhibitors or carbapenems (Dedeic-Ljubovic *et al.* 2010). Isolates of ESBL producing *E. coli* and *Klebsiella* strains are common from UTIs (Ogbolu *et al.* 2018).

2.3.2 *tetA* gene provide bacteria with efflux pumps that is regulated by the *tetR* gene

From 1950 to 2001, the number of human isolates of *E. coli* with tetracycline resistance genes have increased 0.45 % each year and the high consumption of tetracycline in the livestock section throughout the years is one explanation for the rapid spread of resistance genes (Tadesse *et al.* 2012).

The *tet* operon that provides *E. coli* with resistance against tetracycline consists of the genes *tetA* and *tetR* (Muthukrishnan *et al.* 2012). Translation of *tetA* provides bacteria

with an active efflux pump that protects against tetracycline by transferring the antibiotic into the periplasm from the cytosol where transportation is mediated by the release of a proton (Møller *et al.* 2016). In Denmark, TetA has been reported as the most frequently occurring efflux pump against tetracycline in clinical and commensal animal isolates of *E. coli* (Møller *et al.* 2016).

TetR promotes repression of *tetA* and thereby decreases the production of efflux pumps (Møller *et al.* 2016). If no tetracycline is present, TetR is bound to the regulatory sites of *tetA* and *tetR* preventing expression (Muthukrishnan *et al.* 2012). *tetR* expression has been reported to be regulated by tetracycline at concentrations below the minimal inhibitory concentration (MIC) to prevent high energy demanding expression of efflux pumps (Møller *et al.* 2016). At higher concentrations, tetracycline effectively binds to TetR preventing *tetA* repression through a conformational change in TetR that causes TetR to release (Muthukrishnan *et al.* 2012).

2.3.3 Mutation of *dhfr* decrease the interaction with trimethoprim

Trimethoprim binds to the active site of the dihydrofolate reductase (DHFR), an enzyme that is vital in the synthesis of folic acid (Heikkilä *et al.* 1993). Mutations in the DHFR enzyme lead to decreased affinity between the enzyme and trimethoprim. *dhfrXII* is a resistant version of *dhfr* that confers strains with resistance against trimethoprim (Heikkilä *et al.* 1993). The integration of chromosomal *dhfr* genes, including *dhfrXII* into integrons have promoted the spread of the resistance genes between microorganisms through HGT (Wróbel *et al.* 2020). Around 30 integron-associated genes that lead to trimethoprim resistance have been identified that originate from a variety of mutations (Wróbel *et al.* 2020).

2.3.4 Acetyl- and adenyltransferase confer resistance against aminoglycosides

Aac(6')-Ib-cr is an aminoglycoside acetyltransferase commonly located on plasmids and targets aminoglycosides as well as hydrophilic fluoroquinolones (Frasson *et al.* 2011). A secondary amine in the piperazine group of the fluoroquinolone ciprofloxacin is N-acetylated by Aac(6')-Ib-cr and decreases the efficiency of the antibiotic (Park *et al.* 2006). The rapid spread of *aac(6')-Ib-cr* that provides a relatively low grade of resistance in Enterobacteriaceae such as *E. coli* and *K. pneumoniae* still causes concern since it promotes selection of mutants with higher resistance (Frasson *et al.* 2011). AadA2 is an aminoglycoside adenyltransferase that confers resistance against the aminoglycosides streptomycin and is commonly found in *Salmonella* strains (Michael *et al.* 2005).

2.3.5 Mutated *sul-1* lead to decreased affinity towards sulfonamides

sul-1 encodes an dihydropteroate synthase (DHPS) enzyme that is resistant to sulfonamide antibiotics (Antunes *et al.* 2005). DHPS uses PABA as a substrate in the folic acid synthesis (de Castro Spadari *et al.* 2021) and mutations in *sul-1* lead to decreased affinity for sulfonamides with high sequence similarity to PABA. The gene has been associated with integrons and was initially discovered in *Salmonella* (Antunes *et al.* 2005). The most common genes of sulfonamide resistance are *sul-1* and *sul-2* (Antunes *et al.* 2005). Human, livestock and aquaculture *sul-1* isolates have been discovered in a variety of countries (Jiang *et al.* 2019). Antunes *et al.* identified *sul-1* in 76 % of the 200 sulfonamide resistant isolates from clinical and food samples.

2.3.6 *mphA-mrx-mphR* gene cluster causes macrolide antibiotic resistance

The gene cluster *mphA-mrx-mphR* inhibits macrolides with 14-membered rings such as erythromycin (Poole *et al.* 2006). Erythromycin is inactivated by the phosphotransferase MphA through phosphorylation (Poole *et al.* 2006). The function of *mrx* has not been clarified but the expression of *mphA* is dependent on Mrx and MphR is a repressor that downregulates the expression of *mphA* (Poole *et al.* 2006). From 1982 to 2001, the number of animal isolates of *E. coli* with *mphA* resistance genes against erythromycin have increased 1.17 % each year (Tadesse *et al.* 2012).

2.4 The need for new antimicrobial treatment options

Today, the majority of infections caused by bacteria can be cared for by accessible antibiotics or a combination of different antibiotics (Zinner 2007). However, the development of improved antibiotics with broader spectrum and higher efficiency is facing challenges due to the lack of available modification sites and has stagnated over the last years (Singh *et al.* 2017). In addition, the increasing levels of antibiotic resistance and the concerning increase in the number of multiresistant bacteria with limiting clinical treatment options have encouraged the exploration of new antimicrobial options (Zinner 2007). One way to decrease the use of antibiotics is to develop probiotic bacteria that consort protection against pathogens (Henker et al. 2007). The mechanisms of how different types of probiotics work is yet to be clarified and further investigation is needed. Contact-dependent growth inhibition (CDI) systems is one example of how bacteria use toxins to communicate with kin cells (expressing immunity proteins) or to compete with other species (Virtanen *et al.* 2019). Probiotic bacteria could potentially be armed with CDI systems,

making them more effective, however they would still be able to contribute to the spread of antibiotic resistance genes through HGT.

2.5 CRISPR-Cas9 systems protect bacteria against foreign DNA

Through comparative genomic analysis, the understanding of defence systems such as toxin-antitoxin and CRISPR-Cas systems in prokaryotic organisms have increased rapidly (Makarova *et al.* 2013). Some bacteria naturally carry RNA-guided defence systems against transfer of plasmids and infection of phages (Jiang & Doudna 2017). The CRISPR-Cas9 system being one example, has been remodelled in order to develop a dynamic tool for genome editing using only a single guide RNA and the Cas9 protein. CRISPR-Cas9 tools have the potential to aid in the treatment of multiple diseases, including cancer, cystic fibrosis and immunological conditions.

The CRISPR-Cas9 system is a type II system, meaning that the CRISPR loci encodes three Cas proteins; Cas1, Cas2 and Cas9 and sometimes an additional protein, Csn2 or Cas4 (Gupta *et al.* 2019). The first step in the activation of the type II adaptive immune system is the process of immunisation, where small pieces of foreign genetic material are integrated into the chromosomal CRISPR array (Jiang & Doudna 2017). The small sequences classified as spacers are acquired during phage infections collectively by Cas1, Cas2, Cas9 and Csn2 and are integrated into a CRISPR array containing palindromic repeat sequences (Gupta *et al.* 2019). The array is preceded with a leader sequence which provides directionality in the integration process as new spacers are incorporated adjacent to the leader (Gupta *et al.* 2019). A protospacer adjacent motif (PAM) in short proximity to the protospacer is crucial in the integration process (Jiang & Doudna 2017). After integration, the short fragments are allocated at a position between CRISPR repeats and are utilized by the system as memory sequences to prepare for future transfers of the same genetic sequences (Jiang & Doudna 2017).

During invasions of genetic material, the CRISPR array with repeat and spacer sequences is transcribed into a precursor CRISPR RNA (pre-crRNA) (Jiang & Doudna 2017). After transcription, the pre-crRNA is modified through a series of maturation steps (Jiang & Doudna 2017). RNase III cleaves the pre-crRNA into sequences of a single spacer followed by one tracrRNA bound repeat sequence and the spacer sequence is further matured through nuclease activity to a final length of 20 nt (Jiang & Doudna 2017). The spacer that was once integrated to the CRISPR array as a memory of the foreign genetic material is positioned at the 5’ end of the mature crRNA and the 3’ end of the crRNA consists of a CRISPR repeat that is complementary to a trans-activating crRNA (tracrRNA) sequence, coincidently transcribed (Jiang & Doudna 2017). The

mature crRNA forms a complex with the tracrRNA and the Cas9 protein and through the binding of the crRNA to the complementary sequence (protospacer) in the invading genetic material the nuclease activity of Cas9 can be triggered (Figure 2) (Jiang & Doudna 2017). The PAM next to the protospacer is essential for the recognition and destruction of the invading nucleic acid (Jiang & Doudna 2017). Following sequence recognition, Cas9 creates a double-stranded cut in the foreign DNA and thereby protects the cell from DNA uptake.

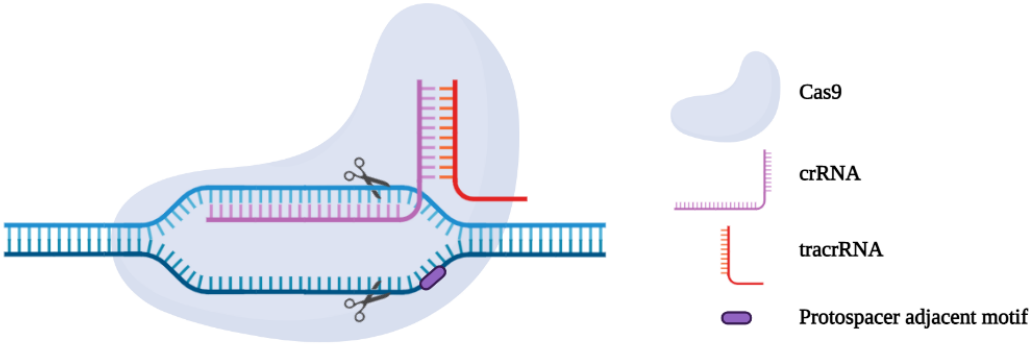

Figure 2: In the destruction of foreign genetic material by CRISPR-Cas9 systems, the crRNA-tracrRNA duplex together with Cas9 locate the protospacer on the incoming DNA and Cas9 performs a double stranded cut in the DNA. The protospacer adjacent motif is crucial for the recognition of the complementary sequence and the endonucleolytic activity of Cas9. Created with BioRender.com

2.6 Previous work

In a previous master thesis project, A. Lundholm (2021) worked with a *S. typhimurium* strain with an existing CRISPR type I system. The CRISPR array in this specific strain consists of spacers against antibiotic resistance genes on the pUUH239.2 plasmid, that is; *ctx-m-15* (cephalosporins), *tetA* (tetracyclines), *oxa-1* (β-lactams), *addA2* and *aac-(6')-Ib-cr* (aminoglycosides), *mrx-2/4* (macrolides), *dhfrXII* (trimethoprim) and *sul-1* (sulfonamides). In order to improve the targeting of antibiotic resistance genes, sequence alignments of the antibiotic resistance genes from different species were made to find conserved regions. In this way, new spacer sequences were designed and the CRISPR array was finally synthesized by Thermofisher on a GeneArt vector (Figure 3).

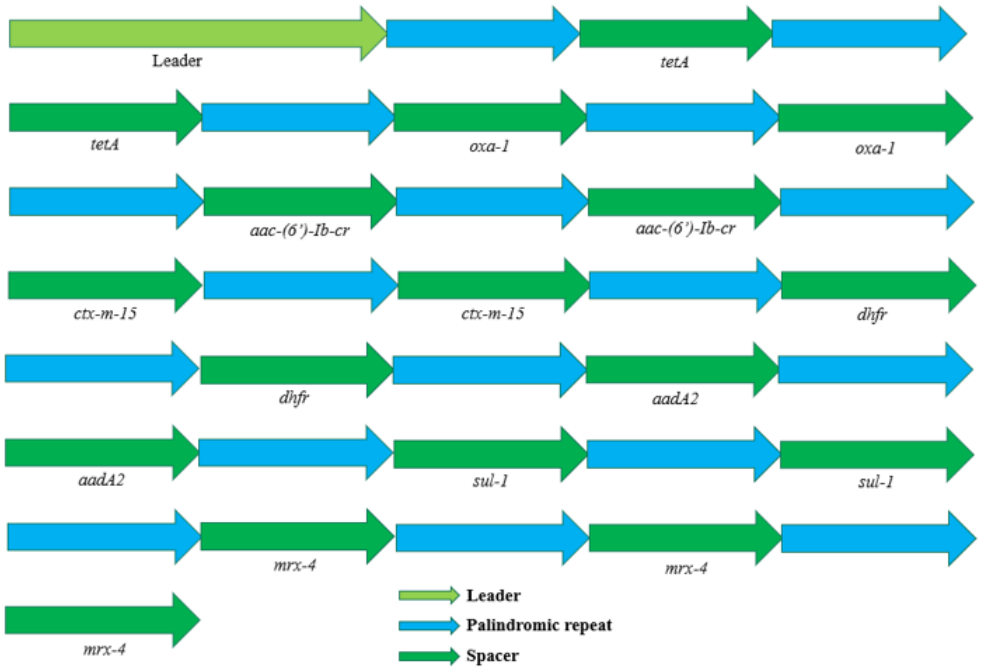

Figure 3: The figure presents an overview of the synthetically constructed CRISPR array.

2.7 Aim of project

In this project, the improved CRISPR array will be further used to create a CRISPR-Cas9 system that can be transferred to the probiotic strain and tested for the protection against transferrable antibiotic resistance genes. The fact that the CRISPR-Cas9 system solely uses one protein for nuclease activity brings an important advantage over a type I system that entails more components in order to function. A CRISPR-Cas9 system is therefore easier to transfer between different strains and is therefore suitable for the probiotic strains that are being developed.

The aim of the project is to investigate whether active CRISPR-Cas9 systems can protect probiotic strains against horizontal transfer of resistance genes. The potential of this specific system protecting the strains from horizontal transfer of the most common antibiotic resistance genes will be tested. The project will study spacers against the following resistance genes; *ctx-m-15* (cephalosporins), *tetA* (tetracyclines), *oxa-1* (beta-lactams), *addA2* and *aac-(6')-Ib-cr* (aminoglycosides), *mrx* (macrolides), *dhfrXII* (trimethoprim) and *sul-1* (sulfonamides). These genes are included on the multiresistant plasmid that was spread during the outbreak at the Uppsala University Hospital (Sandegren et al. 2012).

The difference in how the resistance genes enter the cells and whether that affects the efficiency of the system will also be studied. The project intends to investigate if the number of resistance genes on the foreign genetic material plays a role in the efficiency of the system. The different processes of HGT, that is; conjugation, transformation and transduction will be used to investigate how often antibiotic resistance genes are transferred and whether the presence of the CRISPR-Cas9 system will change the frequency of transfer. A decrease in efficiency is a signal that antibiotic resistance will take longer to develop which is positive for probiotic strains that potentially could be used to treat infections.

The constructed system can be compared to other types of existing systems and in the long run, the project can potentially aid in reducing the spread of antibiotic resistance genes. Potentially such a system could be expanded to prevent probiotic strains from becoming drug resistant or from acquiring virulence genes such as toxins that would transform them into pathogens.

3 Material and methods

3.1 List of strains

Strains from SK lab, referred to in this study are stored in DMSO stock at -80 °C. All strains are listed and described in Table 1. All strains with the execption of SK4668 and SK4669 are derivatives of *E. coli*.

3.1.1 Culture and growth conditions

All cell cultures throughout this project, unless stated otherwise, were prepared in lysogeny broth (LB) media and grown at 37 °C under shaking (200 rpm). The working concentrations of antibiotics were the following; 100 mg/L ampicillin, 50 mg/L kanamycin and 25 mg/L chloramphenicol. The selective Luria–Bertani Agar (LA) plates that were used throughout this study were made according to the following concentrations; 50 mg/L ampicillin, 50 mg/L kanamycin, 15 mg/L tetracyline, 250 mg/L erythromycin, 50 mg/L trimethoprim and 10 mg/L cefotaxime.

Table 1: The table lists all bacterial strains used in this study

List of strains		
Name	**Description**	**Antibiotic reisistance**
SK2	E.coli (Eco) K12 MG1655, wild type	
SK430	Eco K12 MG1655 /pWEB-TNK	ampR, camR
SK891	Eco MG1655 DELsspB	ampR, camR
SK1706	dapA::cat DA38821	camR
SK2629	BW25113 ds-lacA::CefoR	cefoR
SK3524	Eco DELdap /pUUH239.2	cefoR
SK3786	BW25113 ds-lacA::CefoR	cefoR
SK4668	Sty_del(CRISPR1-cas1)::spcdel(CRISPR2)::FRTscar/pJNEG04(miniF, YFP-CTX_M_15-(del bp 98747-44123))	cefoR
SK4669	Sty_del(CRISPR1-cas1)::spc del(CRISPR2)::FRTscar/pJNEG02(miniF, YFP-tetRA(del bp 98747-44123))	tetR
SK4747	DH5alpha /pCRISPathBrick	camR
SK4768	p15a-cas9deg-amp	ampR
SK4869	NEB /pMX-CRISPR array synth	kanR
SK5384	Eco, lacIZYA::FRT, galK::sYFP2-amp, dapA::cat, rifR /plasmid	camR, ampR, cefoR, rifR
SK5385	Eco, lacIZYA::FRT, galK::sYFP2-amp, dapA::cat, rifR /plasmid	camR, ampR, cefoR, rifR
SK5386	Eco, lacIZYA::FRT, galK::sYFP2-amp, dapA::cat, rifR /plasmid	camR, ampR, cefoR, rifR
SK5387	Eco, lacIZYA::FRT, galK::sYFP2-amp, dapA::cat, rifR /plasmid	camR, ampR, cefoR, rifR
SK5388	Eco, lacIZYA::FRT, galK::sYFP2-amp, dapA::cat, rifR /plasmid	camR, ampR, cefoR, rifR
SK5389	Eco, lacIZYA::FRT, galK::sYFP2-amp, dapA::cat, rifR /plasmid	camR, ampR, cefoR, rifR
SK5465	Eco MG1655 /pBAD18-kan	kanR
SK5466	Eco MG1655 /pBAD18:bla(CTX-M-15)	kanR
SK5467	Eco MG1655 /pBAD18:bla(TEM-1)	kanR
SK5468	Eco MG1655 /pBAD18:bla(OXA-1)	kanR

continued on next page

Name	Description	Antibiotic reisistance
SK5469	Eco MG1655 /pBAD18-mphA	kanR
SK5470	Eco MG1655 /pBAD18-mrx	kanR
SK5471	Eco MG1655 /pBAD18-mphR	kanR
SK5472	Eco MG1655 /pBAD18-aac(6')-Ib-cr	kanR
SK5473	Eco MG1655 /pBAD18-sul-1	kanR
SK5474	Eco MG1655 /pBAD18-aadA2	kanR
SK5475	Eco MG1655 /pBAD18-dhfr	kanR
SK5476	Eco MG1655 /pBAD18-tetR	kanR
SK5477	Eco MG1655 /pBAD18-tetA	kanR
SK5478	Eco MG1655 galK::SYFP2-FRT ΔbglGFB::dhfr	cefoR
SK5479	Eco MG1655 galK::SYFP2-FRT ΔbglGFB::mph	tmpR
SK5480	Eco MG1655 galK::SYFP2-FRT ΔbglGFB::tetRA	tetR
SK5481	Eco MG1655 /pWEB-TNC::tracr-cas9deg-CRISPR array	ampR, camR
SK5514	Eco MG1655 DELsspB /pWEB-TNC::tracr-cas9deg-CRISPR array	ampR, camR
SK5550	MG1655 dapA::cat /pJNEG02 (miniF, YFP-tetRA(del bp 98747-44123))	tetR
SK5551	MG1655 dapA::cat /pJNEG04 (miniF, YFP-CTX_M_15-(del bp 98747-44123))	cefoR

3.2 List of oligos

The oligos used for PCR-based screening and cloning are listed in Table 2. All oligos were synthesized by Eurofins.

3.3 Cloning of pWEB-TNC::tracr-cas9-CRISPR plasmid

In this section, the construction of the pWEB-TNC::tracr-cas9-CRISPR plasmid will be described. An overview of the final plasmid construct can be seen in Figure 4.

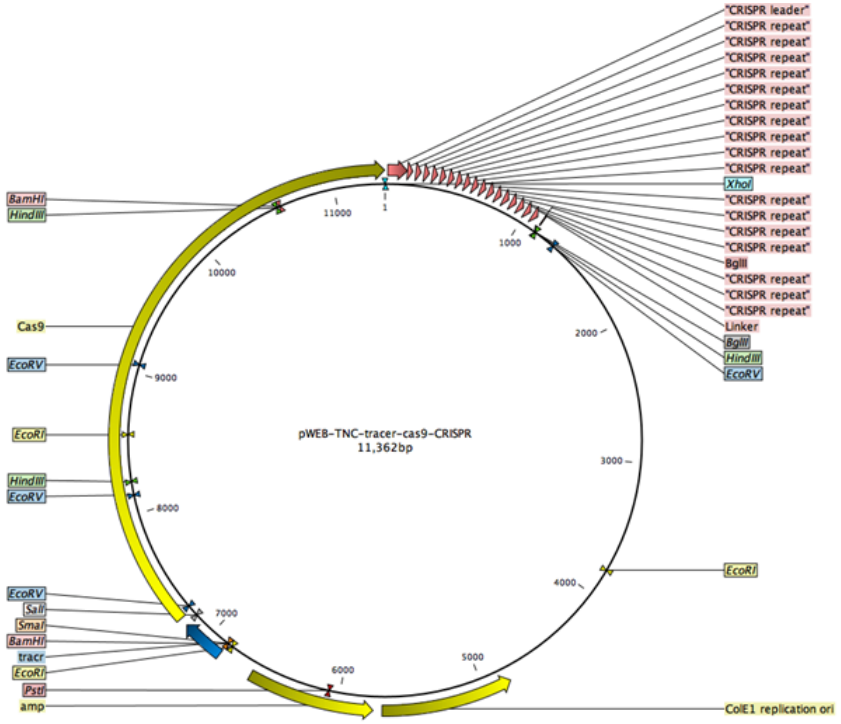

Figure 4: The figure presents an overview of the pWEB-TNC::tracr-cas9-CRISPR plasmid that was constructed. The plasmid backbone contains an ampicillin resistance gene, a chloramphenicol resistance gene (not shown) and an origin of replication. The figure was generated by CLC Bio.

All digestion reactions during the cloning were performed using Thermo Scientific™ FastDigest restriction enzymes and FastDigest buffer (10X). Thermo Scientific™ T4 DNA Ligase (5 U/µL) and 10X T4 DNA Ligase Buffer were used in all ligation steps. The plasmids were prepared using Thermo Scientific™ GeneJET Plasmid Miniprep Kit

Table 2: The table presents all oligo used in this study

List of oligos		
Name	**Sequence**	**Description**
SK1805	gcgcCCCGGGTTACGAAATCATCCTGTGG	tracer_F(smaI)
SK1806	tataGTCGACTCTCCTTGATTATTTGTTATAAAAG	tracer_R(SalI)
SK1807	atatGTCGACTTTACAGCTAGCTCAGTCCTAG-GTATTATGCTAGCGCAATTAGAGGGCT-CAATGG	Cas9_F (SalI)
SK1808	gcgcAGATCTtctagaCTCGAGTTAAGCAGCCAGAG	Cas9_R (BglII)
SK1831	AGTATACTCGAGTTTTAGATGA	F_primer for amplify leaderspacer construct from plasmid
SK1832	gcgcAGATCTGCTAAAACTA	R_primer for amplify leaderspacer construct from plasmid
SK1926	GTGCCACCTGACGTCTAAG	pWEB-TNC_for
SK1927	CATACACGGTGCCTGACTG	pWEB-TNC_rev
SK1929	TCGTTTCATACGCTCTCGCG	cas9_verR
SK1930	AGCAAGATGGCAGCGCCTA	tracer_verF
SK1931	AAGTGGCACCGAGTCGGTG	tracer_verR
SK1985	GATCTGAGGATCATCAGTCGAC	Confirmation reverse primer of linker in pWEB-TNC

continued on next page

Name	Sequence	Description
SK1986	CGAATCTTGGAGCTCCCGC	Confirmation forward primer of CRISPR array in pWEB-TNC, binding at the end of cas9
SK1987	GGGATGATTGTCGACTGATGATCCTCA-GATCTCA	Linker with BgII and SalI
SK1988	AGCTTGAGATCTGAGGATCATCAGTCGACAAT-CATCCC	Linker with BgII and SalI, with BgII overhang

according to the protocol provided by the manufacturer. All PCR products were purified with the Thermo Scientific™ GeneJET PCR Purification Kit in line with the accompanying instructions. NanoDrop® ND-1000 Spectrophotometer was used to measured all plasmid DNA concentrations. All agarose gels were stained with Invitrogen™ SYBR™ Safe DNA Gel Stain (10000X). Thermo Scientific™ DreamTaq DNA Polymerase, recombinant (5 U/µL) and 10X DreamTaq buffer were used in the Taq PCR reactions. For the Phusion PCR reactions, Thermo Scientific™ Phusion™ High-Fidelity DNA Polymerase (2 U/µL) and the 5X Phusion HF buffer were used. All sequencing reactions were performed by Eurofins.

3.3.1 Insertion of linker with BglII and SalI digestion sites

The original pWEB-TNC plasmid was initially extracted from SK430. The pWEB-TNC plasmid was digested with SmaI and HindIII restriction enzymes at 37 °C for 1 h and 40 minutes and the enzymes were heat-inactivated at 80 °C for 10 minutes. The digestion reaction was prepared according to Table A3. The digested product was purified on an agarose gel using the Thermo Scientific™ GeneJET Gel Extraction Kit according to the instructions provided by the manufacturer and the band was visualised and cut out on a UV-screen. The linker oligos SK1987 and SK1988 were aligned in temperature falling reaction according to Table A4. The aligned linker and the digested pWEB-TNC plasmid were ligated at 16 °C for 16 hours and the enzyme was inactivated at 60 °C for 10 minutes. The ligated pWEB-TNC::linker plasmid was transformed into NEB cells according to the protocol described in Section A.1.1. Transformants carrying the correct

insert were identified by PCR according to Table A6 using oligos SK1926 and SK1985 as well as oligos SK1926 and SK1927 followed by sequencing. The pWEB-TNC::linker plasmid was prepared and the concentration of the plasmid preparation was determined. In order to test the inserted restriction sites, digestions of the original pWEB-TNC plasmid and the pWEB-TNC::linker plasmid with SalI and PstI restriction enzymes were performed according to Table A7.

3.3.2 Insertion of the tracr and cas9 sequences

The tracr gene was amplified from SK4747 using Phusion High-Fidelity PCR with oligos SK1805 and SK1806. SK4747 has a pCRISPathBrick vector with a tracrRNA from *S. pyogenes*. The reaction set up can be seen in Table A2 and the PCR program is presented in Table A8. The Cas9 gene was amplified from SK4768 using Phusion High-Fidelity PCR with oligos SK1807 and SK1808. SK4768 contains a plasmid that has a Cas9 gene with an additional degradation tag. Minor adjustments to the protocol in Table A2 were made as 1.25 µl of primers, 0.25 µl of Phusion polymerase were used and 0.25 µl $MgCl_2$ was added to a total volume of 20 µl. As the yield of Cas9 was very low, three separate additional Phusion PCR using a colony, the first PCR and a plasmid preparation of the plasmid from SK4747 as templates were performed (Table A9). The denaturing step was changed to 15 s, annealing temperature was set to 55 °C and the extension time was extended to 3 minutes. The PCR product that used the plasmid as the template was purified.

The pWEB-TNC::linker plasmid, prepared as described in the previous section was digested with restriction enzymes SmaI and BglII. The purified Cas9 was digested with SalI and BglII. SmaI and SalI were used to digest the purified tracr sequence. All products were digested at 37 °C for 1 h and the reaction set up can be seen in Table A10. The digested products were purified and the concentrations of vector, tracr and cas9 were measured. The three digestion products were ligated in a 3:1 molar vector:insert ratio according to Table A11 at 16 °C for 19 hours. The ligated vector was transformed into NEB cells according to the protocol in A.1.1 and selected on ampicillin plates. The colonies were screened for the correct insert using Taq colony PCR with three sets of different primers; SK1926+SK1927, SK1930+SK1929 and SK1926+SK1931. Table A6 shows the PCR program (with an extended elongation time of 5 minutes and 3 minutes for primer sets SK1926+SK1927 and SK1930+1929 respectively). The PCR products were visualised on an agarose gel and clones with the correct sized insert were verified by sequencing.

3.3.3 Insertion of the synthetic CRISPR array

A plasmid preparation of the pWEB-TNC::tracr-Cas9 construct described in the previous sections was made and the concentration was measured. The plasmid with the synthetic CRISPR array was extracted from SK4869 and the concentration was measured. Both plasmids were digested with BglII and Xhol restriction enzymes according to Table A12 at 37 °C for 1 hour. The digested products were purified and the concentrations were measured. The products were ligated in a 3:1 vector:insert ratio according to Table A13 for 20 hours 37 °C and the enzymes were heat-inactivated for 10 minutes at 60 °C. The ligated plasmid was transformed into NEB cells according to the protocol described in A.1.1 and selected on ampicillin plates. The colonies were screened for the CRISPR insert using Taq colony PCR with primers SK1986 and SK1927 according to the PCR program in Table A6. The PCR products were visualised on an agarose gel and clones with the correct sized insert were verified by sequencing.

3.4 Testing of the CRISPR-Cas9 system

3.4.1 Transformation of the pWEB-TNC::tracr-cas9-CRISPR plasmid into test strains

The pWEB-TNC::tracr-cas9-CRISPR plasmid was transformed into a wild type *E. coli* MG1655 (SK2) by sweaping up colonies from a plate using a cotton swab into a pre-chilled eppendorf tube with 500 µl of ice cold 10 % glycerol. The cell mix was washed one time with 500 µl of ice cold 10 % glycerol and 50 µl of the mixture together with 1 ul of the pWEB-TNC::tracr-cas9-CRISPR plasmid preparation was added to an electroporation cuvette. The cells were electroporated at 1.8 kV, 225 Ω and 25 25 µF and recovered in 500 µl of LB medium for one hour. The cell mix was selected on ampicillin plates at 37 degrees.

The pWEB-TNC::tracr-cas9-CRISPR plasmid was transformed into *E. coli* MG1655 Δ*sspB* (SK891), lacking the *sspB* gene that is necessary in order to recognise the SsrA degradation tag on the Cas9 protein by performing a 1:100 dilution of an 5 ml overnight culture into 50 ml of LB medium and incubation of the culture for 1 hour at 37 °C (200 rpm). The cell mixture was centrifuged for 7 minutes, 3000 rpm at 4 °C and washed with 25 ml of 10 % glycerol. The pellet was washed one more time with 25 ml 10 % glycerol and sequentially resuspended in 1 ml of 10 % glycerol and centrifuged at 6000 rpm for 3 minutes at 4 °C. Finally, the pellet was resuspended in 200 µl of 10 % glycerol and 50 µl was alliqouted with 1 µl of DNA into electroporation cuvettes. The electroporation was performed as previously described.

3.4.2 Test of transformation frequencies

Plasmids with the single resistance genes on the pBAD18 vector from SK5465-SK5477 were prepared from overnight cultures. 2 ml of LB medium was inoculated with the test strains +/- CRISPR plasmid and incubated at 37 °C overnight. A 1:100 dilution in tubes (one for OD_{600} measurements) of 5 ml LB (with ampicillin for the +CRISPR strain) was incubated at 200 rpm until an OD_{600} of 0.4-0.6 was reached. The cells were spinned down at 3000 rpm for 10 minutes and the pellets were resuspended in 150 µl of cold LB. 150 µl of 2x TSS was added and 105 µl was transferred into a ice-chilled falcon tube. The cell mixtures were incubated on ice for 5 minutes and 150 ng of DNA was added. The DNA was mixed with a pipette tip and the cells were kept on ice for 30 minutes. 900 µl of 1x TSS with 0.02 % glucose was added to the cell mixtures. The cells were shaken at 37 °C for 1 hour. The cell mixtures were plated on kanamycin plates and 10-fold dilution series were spotted on LA plates as well as kanamycin plates. The plates were incubated at 37 °C for 16-18 hours. The relative transformation frequencies were calculated by dividing the cfu multiplied with the dilution factor d divided by the plated volume, according to Formula 1.

$$\textit{Frequency of transfer} = \frac{\frac{cfu_{selective}d}{V}}{\frac{cfu_{LA}d}{V}} \tag{1}$$

3.4.3 Test of transduction frequencies

Lysates of SK5478-SK5480 and SK2629 were prepared by mixing 20 µl of overnight culture with 2 ml of LB medium and 10 µl of 1M $CaCl_2$. The cell mixtures were incubated at 37 °C for 1 hour and 20 µl of P1 lysate (MG1655) was added. The mixtures were incubated at 37 °C for 4 hours. Cells were separated from lysate by centrifuging the mixes for 1 minute at 13 000 rpm and the supernatants were filtered into 2 ml eppendorf tubes.

The transductions were performed by spinning down 5 ml overnight cultures at 3000 rpm for 10 minutes. The cells were resuspended in 1 ml LB with 10 mM $MgSO_4$ and 5 mM $CaCl_2$. 100 µl of cells were mixed with 50 µl of the prepared P1 lysates and incubated at 30 °C for 30 minutes. 1 ml of LB medium with 0.1 M sodium citrate was added and the cells were incubated at 37 °C for 1 hour. The cell mixtures were plated on kanamycin plates and 10-fold dilution series were spotted on LA plates as well as kanamycin plates. The plates were incubated at 37 °C for 16-18 hours. The transduction frequencies were calculated in the same way as the transformation frequencies as seen in Formula 1.

3.4.4 Test of conjugation frequencies

100 µl of each overnight culture (donor and recipient) were mixed and spun down for 5 minutes at 6000 rpm. The cells were resuspended in 50 µl of the supernatants and spotted onto LA plates. The plates were incubated at 37 °C for 3-4 hours. The conjugation mixtures were swabbed into 1 ml of PBS and plated as well as spotted on selective plates. The plates were incubated at 30 °C for 16-18 hours. The conjugation frequencies were calculated in the same way as the transformation and transduction frequencies as seen in Formula 1.

3.4.5 Western blot of Cas9 levels

Cell cultures were grown to an OD_{600} of 0.38-0.51 and cells corresponding to an OD600 of 1 were harvested by centrifugation at 13 000 rpm for 1 minute. The cells that were prepared for TSS treatment were resuspended in 150 µl of ice cold LB. 150 µl of 2x TSS buffer was added and the cells were incubated on ice for 5 minutes. 900 µl of 1x TSS with 0.01 % glucose was added to the mixtures and the cells were incubated in 37 °C for 5 minutes. The cells were harvested by centrifugation at 13 000 rpm for 1 minutes. The TSS-treated and non-treated pellets were dissolved in 25 µl LDS and 25 µl of water. The tubes were incubated at 95 °C for 5 minutes and 0.5 µl of benzonase was added followed by an incubation at room temperature for 10 minutes. 10 ul of the samples was loaded onto a 2D TRIS-acetate gel. The proteins were transferred from the gel using the Invitrogen™ iBlot™ 2 Gel Transfer Device at 20 V for 10 minutes and 23 V for 3 minutes. The membrane was incubated for 1 hour under shaking in milk-TBS solution (5 % milk). The primary Cas9 antibody (Cas9 Monoclonal Antibody (7A9) - MA5-23519) in a 1:4000 dilution was added and the membrane was incubated at room temperature under shaking for 16 hours. The membrane was washed two times for 5 minutes under shaking with TBS buffer. The secondary antibody (anti-mouse) was added in a 1:4000 dilution to milk-TBS solution (5 % milk) and incubated under shaking for 1 hour. Four additional washing steps of 5 minutes under shaking were performed before the membrane was scanned. The reference protein (RNA polymerase B) was added in a 1:4000 dilution and the membrane was incubated under shaking for 1 hour. The membrane was washed two times with TBS under shaking and the secondary antibody was added in a 1:4000 dilution to milk-TBS solution (5 % milk). Four additional washing steps of 5 minutes under shaking were performed before the membrane was scanned.

4 Results

4.1 Cloning of pWEB-TNC::tracr-pJ23101cas9deg-CRISPR synthetic plasmid

To be able to investigate if the presence of a CRISPR-Cas9 system can change the frequency of transfer of antibiotic resistance genes, a plasmid containing the tracr, Cas9 and CRISPR array sequences was constructed. The pWEB-TNC plasmid, was chosen as the backbone of the system and was extracted from the SK430 strain with a concentration of 189.3 ng/µl. First, a linker sequence with additional restriction sites was added to the pWEB-TNC plasmid to be able to include the tracr, Cas9 and CRISPR array sequences to the plasmid. The concentration of the aligned linker was measured to 1700 ng/µl. In order to confirm the linker insert, colonies were screened by PCR. Oligos binding in the vector were used (SK1926 and SK1927) where a small (37bp) decrease in the expected size of the amplified fragment was expected. 12 of 15 transformants showed a small decrease in band size (Figure A.1), but the small difference was difficult to observe on the gel so a second PCR was set up where the transformants were screened using one oligo binding in the vector (SK1926) and one that binds in the linker (SK1985). The expected product (157bp) was identified in 14 of the transformants (Figure A.2). Sequencing results from Eurofins showed that the product had a successful insertion of the linker sequence with BglII and SalI restriction sites. In addition, a test digest of the pWEB-TNC::linker plasmid using two different pairs of restriction enzymes (one in each pair corresponding to the restriction sites in the linker sequence) was performed. Two bands of the correct sizes (799 and 4976 bp) on an agarose gel were observed for the four tested samples and confirmed the added restriction sites in the linker (Figure A.3).

Next, the tracr and Cas9 sequences were amplified by PCR from SK4747 (with primers SK1805+SK1806) and SK4768 (with primers SK1807+SK1808) respectively. A ssrA degradation tag that is recognized by strains expressing the SspB protein by which the protein is marked for degradation was added to the Cas9 protein. The degradation tag was added to the protein in order to keep the amount of protein in the cells to a moderate level as it is expressed under a strong constitutive promoter (J23101).

The amplified PCR products (tracr Figure A.4 and Cas9 Figure A.5) were verified for correct sizes (291 bp and 4164 bp for tracr and Cas9 respectively) using gel electrophoresis. As seen in Figure A5, the yield of the first Cas9 PCR product was low and was therefore used as a template in a second nested PCR. The nested PCR resulted in sufficient amounts of cas9 gene product for cloning with a concentration of 94.3 ng/µl (Figure

A.6). The PCR products as well as the pWEB-TNC::linker vector were digested and purified. The concentrations of vector, tracr and cas9 were measured to 36.8, 1.7 and 39.2 ng/µl respectively. Successful transformants were screened for correct insert using oligos binding in the vector (SK1926+1927) and in cas9 (SK1929) for cas9 and in the tracr (SK1930+SK1931) for tracr. Three different cloning experiments, of which two separately cloned the tracr and cas9 into the vector and one performing a double insertion of the two sequences in a single-step manner were performed. Two transformant from the single-step cloning showed the correct size of 4696 bp (Figure A.7 and A.8) and were used for the next step where the synthetic CRISPR repeats were inserted into the vector by restriction digestion and ligation. The plasmid with the synthetic CRISPR array was extracted and the concentration was measured to 147.1 ng/µl. The plasmid with the CRISPR array along with the pWEB-TNC::tracr-cas9 plasmid were digested and purified and the concentrations were measured to 30.9 and 16.1 ng/µl respectively. Successful transformants from the final cloning were screened using oligos binding in the constructed vector (SK1931 and SK1932). 7 out of 11 transformant had the correct size of 1388 bp (Figure A.9) and two of these colonies were verified by sequencing of the tracr, Cas9 and the CRISPR array sequences to confirm the correct insertion in the final pWEB-TNC::tracr-pJ23101-cas9deg-CRISPRsynthetic plasmid construct (from now on referred to as the CRISPR plasmid).

The constructed CRISPR plasmid was transformed into MG1655 (SK2) and the MG1655Δ*sspB* strains to test the frequency of resistances gene transfer through transformation, transduction and conjugation and compare the results to the corresponding wild type strains (-CRISPR plasmid). The MG1655Δ*sspB* strain lacks the SspB protein that recognizes the ssrA degradation tag on the Cas9 sequence and was included in the experiment to investigate if the level of Cas9 in the cells affects the efficiency of the CRISPR-Cas9 system.

4.2 Transformation frequency of resistance genes into MG1655 and MG1655Δ*sspB* +/- CRISPR plasmid

To test the efficiency of the CRISPR-Cas9 system on single resistance genes, bacteria were transformed with pBAD18 plasmids containing single resistance genes from the pUUH239.2 clinical plasmid. As negative controls, *mrphA, mphR, tetR, tem-1* and a kanamycin resistance gene were used and the transformation frequency was measured in wild type MG1655 (SK2) and MG1655 with the CRISPR plasmid (SK5481). The transformation frequencies were measured by comparing the colony forming units per ml (cfu/ml) on the selective plates to the cfu/ml on LA plates according to Formula 1. The negative control genes without matching spacer sequences; *mrphA, mphR, tetR,*

tem-1 and a kanamycin resistance gene showed no visible difference in transformation frequency between the two strains (Figure 5). All except two, *tetA* and *sul-1* of the genes that have corresponding spacer sequences on the CRISPR array showed no significant difference in transformation frequency. A 32-fold difference and 100-fold difference in transformation frequency between the MG1655 and MG1655 with the CRISPR plasmid was observed for *tetA* and *sul-1* respectively.

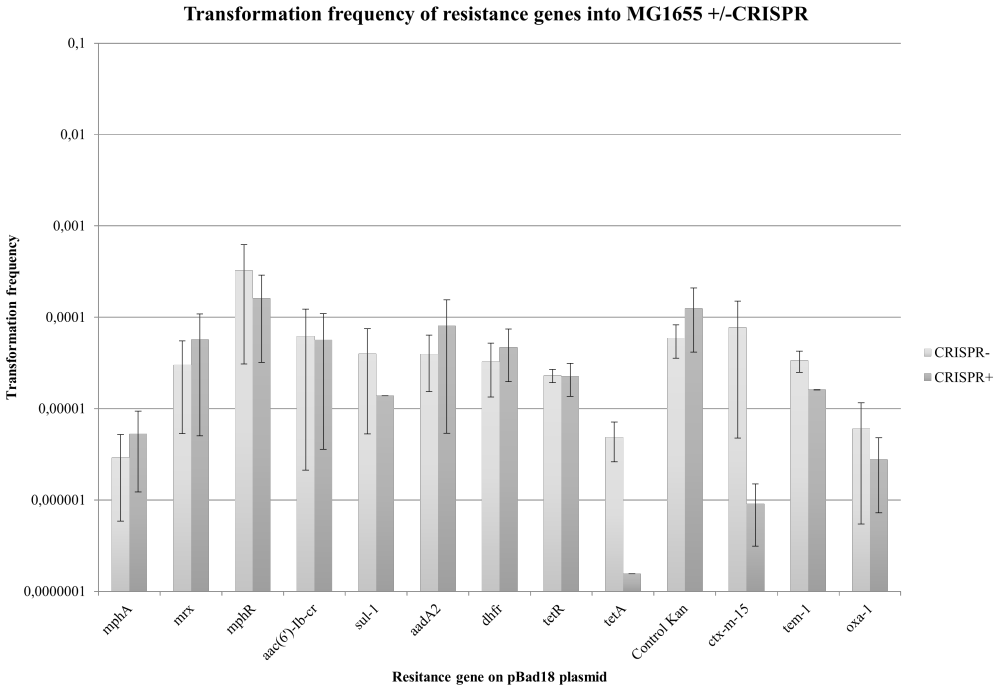

Figure 5: The figure presents the results from the transformation assays with pBAD18 plasmids with single resistance genes from the clinical plasmid pUUH239.2 into wild type MG1655 and MG1655 with the CRISPR plasmid. The CRISPR array contains spacers corresponding to mrx, aac(6')-Ib-cr, sul-1, aadA2, dhfr, tetA, ctx-m-15 and oxa-1. n = 2.

To investigate if the difference in transformation frequency of MG1655 and MG1655 with the CRISPR plasmid would increase if the levels of Cas9 protein in the cells increased, the same experiment using an MG1655 strain lacking the SspB protein that promotes degradation of the ssrA tag on the Cas9 protein (SK891) and the same strain with the CRISPR plasmid (SK5514) was performed. In this way, the proposition whether or not the level of Cas9 protein makes a difference in the efficiency of the system was investigated. The objective behind this experiment was that decreased levels of Cas9 degradation in the cells will make more Cas9 protein available and active for degradation of the incoming resistance genes. Similarly to the transformation assay with wild

type MG1655, the negative control genes without matching spacer sequences; *mrphA, mphR, tem-1* and a kanamycin resistance gene showed no visible difference in transformation frequency between the MG1655Δ*sspB* +/- CRISPR plasmid strains (Figure 6). The MG1655Δ*sspB* + CRISPR strain showed a lower transformation frequency of *tetR* compared to the MG1655Δ*sspB* strain despite lacking a matching spacer sequence. When comparing the two experiments, *mrx, dhfr* and *tetA* are the genes that have the highest increase in difference of transformation frequency between the +/- CRISPR plasmid strains when the assay is performed in the MG1655Δ*sspB* strain. However, the difference between the MG1655 and MG1655Δ*sspB* strains in transformation frequency for *mrx* and *dhfr* was not significant. In contrast, a significant, 1000-fold difference in transformation frequency was observed for the *tetA* gene in the Ssp- background, as compared to a 100-fold difference in the Ssp+ background. This suggests that the level of Cas9 protein in the cells is important for the efficiency of the CRISPR-Cas9 system.

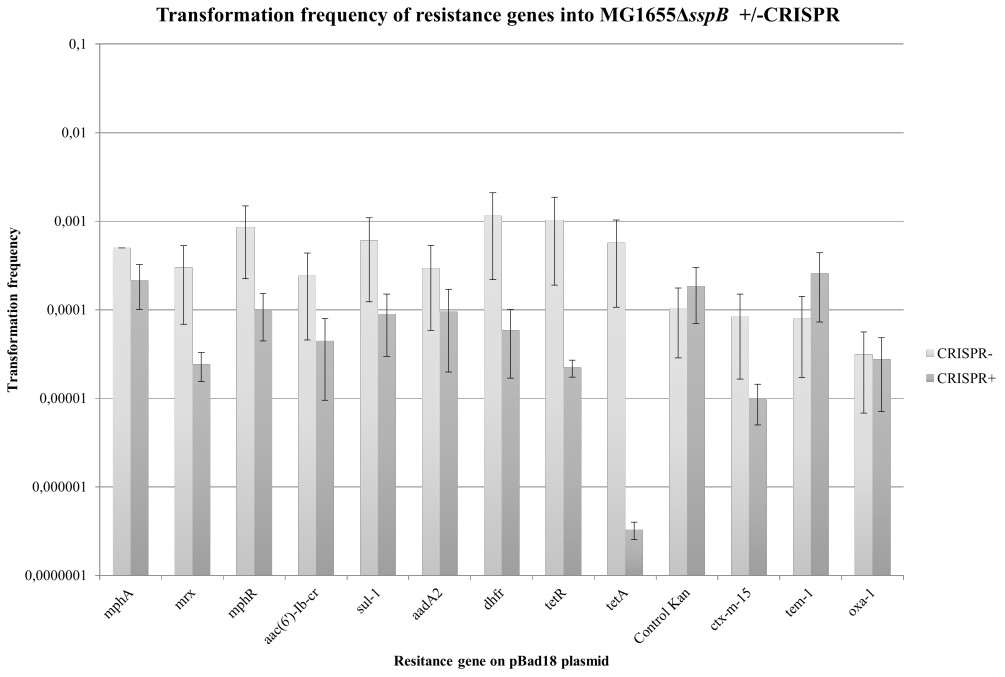

Figure 6: The figure presents the results from the transformation assays with pBAD18 plasmids with single resistance genes from the clinical plasmid pUUH239.2 into MG1655ΔsspB and MG1655ΔsspB with the CRISPR plasmid. The CRISPR array contains spacers corresponding to mrx, aac(6')-Ib-cr, sul-1, aadA2, dhfr, tetA, ctx-m-15 and oxa-1. n = 2.

4.3 Western blot of Cas9 in MG1655 and MG1655Δ*sspB* +/- CRISPR plasmid

To investigate how deletion of the *sspB* gene affects the levels of Cas9 protein in MG1655 strains we used western blot where the Cas9 levels are detected with anti-Cas9 antibodies. In addition, TSS treated samples were analysed to investigate if the treatment used for transformation affects Cas9 expression in cells. In addition, the strain from which cas9 was originally amplified from (SK4768) was used as a positive control. However, no Cas9 could be detected in this strain, possibly due to the lack of promoter induction (pTet). Bands of the correct size (160 kDa) were observed for samples containing our Cas9 construct (Figure 7), suggesting that the antibodies used in the experiment are highly specific to the Cas9 protein. As seen in Figure 7, a small difference in band intensity was observed between the +/- SspB samples, suggesting that the levels of Cas9 in the -SspB samples are higher compared to the wild type samples. In addition, the lower band intensities for the TSS treated samples suggest that the TSS buffer lead to decreased levels of Cas9 in the cells.

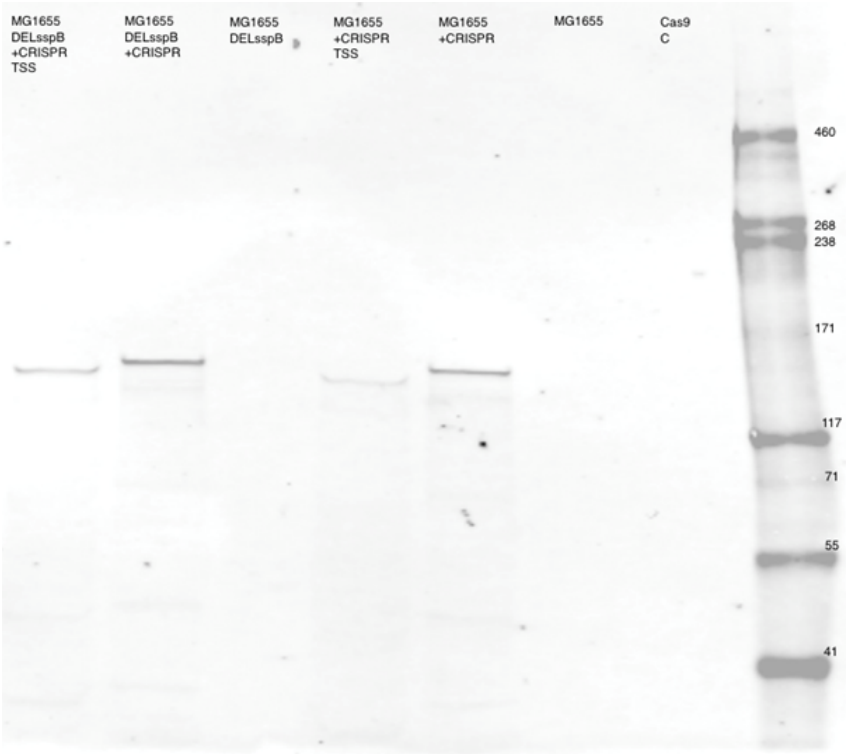

Figure 7: The figure shows the western blot were the levels of Cas9 in the MG1655 as well as the MG1655ΔsspB +CRISPR strains. The same strains were also treated with TSS to analyze if the treatment affects the levels of Cas9 in the cells. SK4768 was used as a positive control and the MG1655 and MG1655ΔsspB strains without the CRISPR plasmid were used as negative controls. Marker: Invitrogen HiMark prestained protein standard.

Even though the optical densities of the cell cultures were measured prior to loading the gel in order to inject the same amount of cells in the wells, there was a possibility that the loaded amount differs between the samples. Therefore, RNA polymerase B (RpoB), that is equally expressed in the samples, was used as a reference. The western blot membrane was incubated with primary and secondary antibodies in order to generate Figure 8. The intension was to quantify the band intensities to see if the deletion of *sspB* or the conditions used for transformation changed Cas9 level, by normalising the levels of Cas9 to the respective RpoB values. However, an exact quantification was not performed due to issues with varying levels of background on the membrane. In conclusion, the results give an indication that the SspB protein in the cells promotes degradation of Cas9, however the levels of Cas9 in the cells needs to be further investigated in order to conclude that the level of Cas9 in the MG1655Δ*sspB* +CRISPR strain is higher compared to the wild type strain.

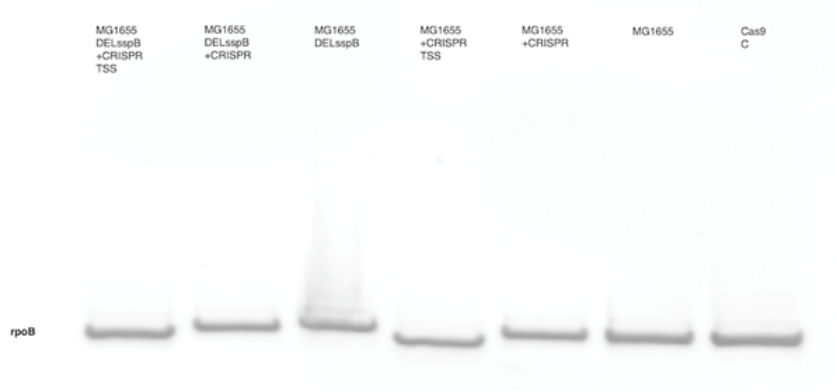

Figure 8: The figure shows the western blot were the levels of RNA polymerase B in the MG1655 as well as the MG1655ΔsspB +CRISPR strains. The RNA polymerase B levels were also estimated in the same strains with TSS treatment. Additionally, the levels of RNA polymerase in the positive control SK4768 and negative controls MG1655 and MG1655ΔsspB strains without the CRISPR plasmid was estimated.

4.4 Transduction frequency of resistance genes into MG1655 and MG1655ΔsspB +/- CRISPR plasmid

Next we set out to investigate how the constructed CRISPR system could protect against HGT of resistance genes through transduction. The MG1655 +/- CRISPR plasmid strains were transduced with P1 lysates of MG1655 with chromosomal *ctx-m-15, dhfr, mph* and *tetRA* (SK2629, SK3786, SK5478-SK5480). The transduction frequencies were measured by comparing the colony forming units per ml (cfu/ml) on the selective plates to the cfu/ml on LA plates according to Formula 1. No significant difference in transduction efficiency was observed between the MG1655 +/- CRISPR plasmid strains for the transductions of *dhfr* despite the matching spacer sequences of the system (Figure 9). In contrast, although the CRISPR array does not contain spacers matching *mph* a 10-fold difference between the two strains was detected for the transductions of *mph*. In agreement with the results from the transformation assay, a 32-fold difference for *tetRA* was observed. For the *ctx-m-15* no colonies could be observed from either transduction and the frequencies could not be calculated. The results indicate that the spacers corresponding to *tetA* seems to have the highest efficiency in resistance gene destruction.

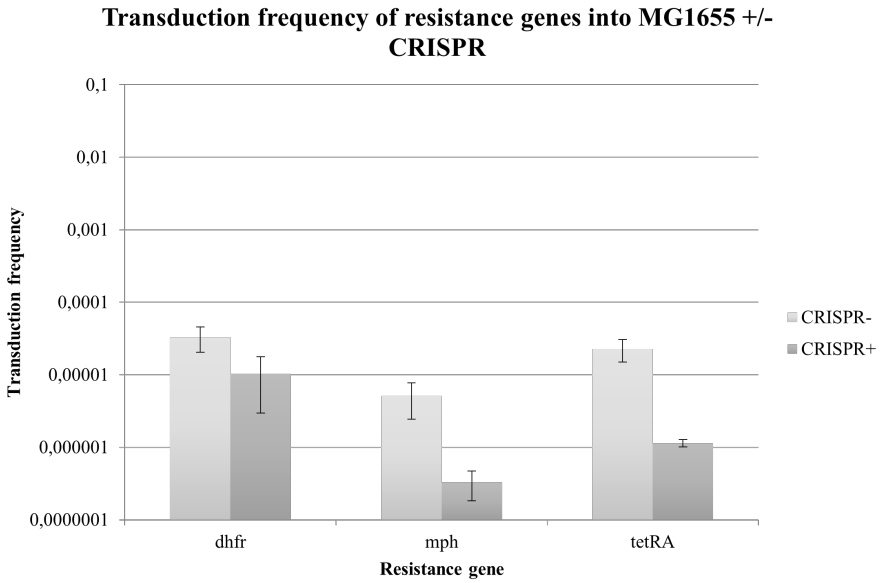

Figure 9: The figure presents the results from the transduction assays with MG1655 chromosomal resistance genes dhfr, mph and tetRA from the clinical plasmid pUUH239.2 into wild type MG1655 and MG1655 with the CRISPR plasmid. The CRISPR array contains spacers corresponding to dhfr and tetA. n = 3.

The same experiment was performed in MG1655Δ*sspB* +/- CRISPR plasmid to investigate if the results in transfer of resistance genes would be consistent with the transformation assay where a larger difference in transformation frequency could be observed between +CRISPR/- strains in Δ*sspB* background compared to that in wild type. In line with the results from the wild type experiment, no distinguishable difference between the +/- CRISPR plasmid strains for *dhfr* was visible (Figure 10). An approximate 100-fold difference between the +/- CRISPR plasmid strains in the cases of *mph* and *tetRA* was observed. This is an increase from the wild type experiment and again indicates that an increased level of Cas9 in the cells promotes the activity of the CRISPR-Cas9 system.

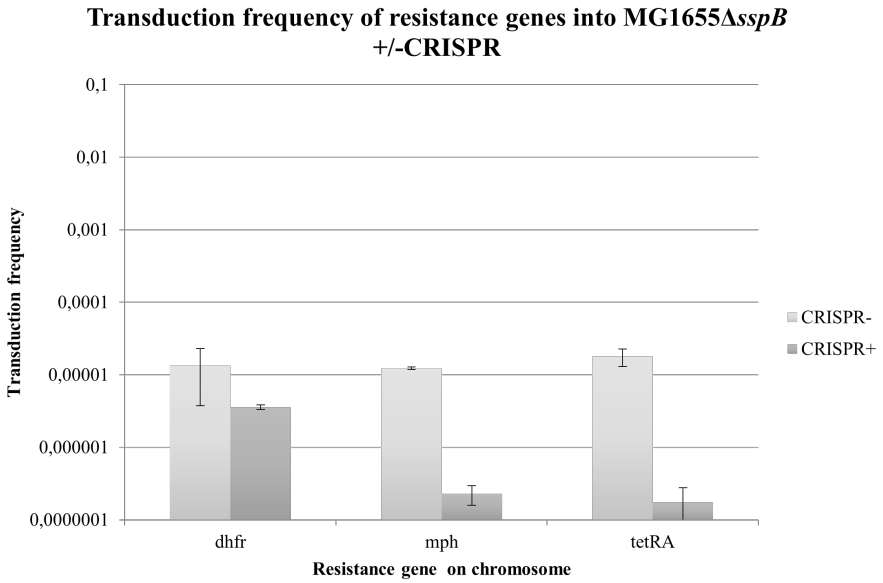

Figure 10: The figure presents the results from the transduction assays with MG1655 chromosomal resistance genes dhfr, mph and tetRA from the clinical plasmid pUUH239.2 into2 into MG1655ΔsspB and MG1655ΔsspB with the CRISPR plasmid. The CRISPR array contains spacers corresponding to dhfr and tetA. n = 3.

4.5 Conjugation frequency of resistance genes into MG1655 and MG1655Δ*sspB* +/- CRISPR plasmid

Conjugation assays in the MG1655Δ*sspB* +/- CRISPR plasmid strains were performed to investigate if the presence of the constructed system can protect bacteria against transfer of single resistance on mini-F plasmids. The results, presented in Figure 11, showed that the system does not protect the bacteria against transfer of *ctx-m-15* and *tet* through conjugation, as no significant difference in conjugation frequency was observed between the MG1655Δ*sspB* +/- CRISPR plasmid strains. When constructing the SK5550 and SK5551 strains for the conjugation experiment the mini-F plasmids with *tet* and *ctx-m-15* resistance genes where conjugated into SK1706 (a DAP::cat strain) from SK4668 and SK4669. The conjugation mixes were plated on DAP+cam plates and restreaked on DAP+cefo and DAP+tet plates respectively. When grown in overnight cultures the constructed strains displayed irregular behavior, sometimes growing in chloramphenicol and sometimes not growing at all. The strains were grown on cam and LA plates to test the *dapA::cat* cassette. Neither of the constructed strains showed growth on cam plates and both of the strains grew on non-selective LA plates. This indicates that there is a

mix in the population of the donor strains where some are dapA::cat and others have the wild type genotype. For this reason, the results in Figure 11 are unreliable since the donor cells with wild type dapA can grow on the LA plates supplemented with antibiotics (CEF/TP/TET) used to select for targets that successfully received the plasmid.

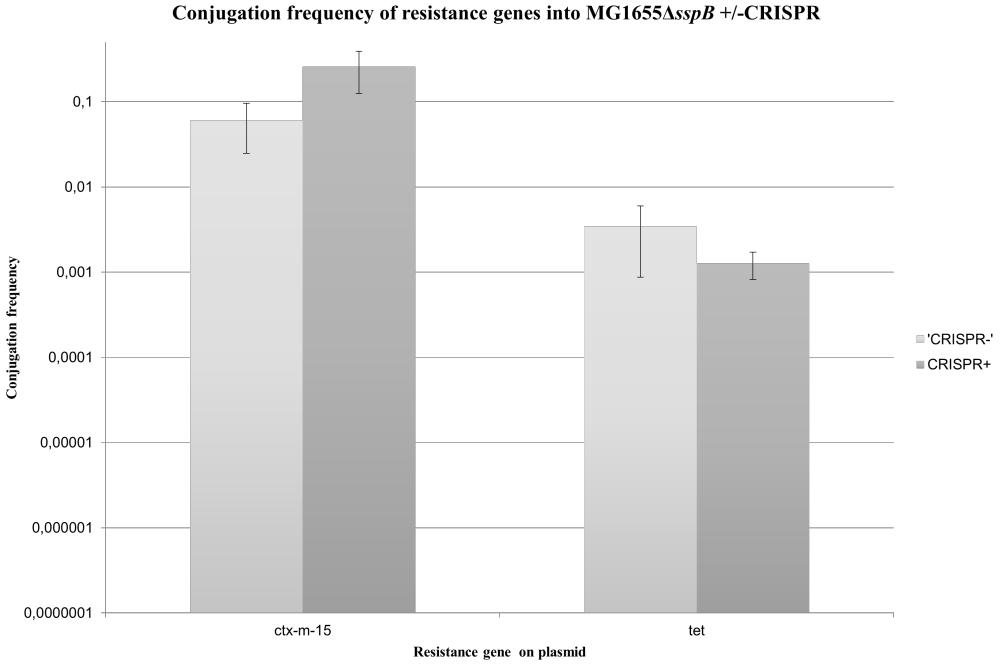

Figure 11: The figure presents the results from the conjugation assays with resistance genes ctx-m-15 and tetA on miniF plasmids into MG1655ΔsspB and MG1655ΔsspB with the CRISPR plasmid. The CRISPR array contains spacers corresponding to both ctx-m-15 and tetA. n = 3.

4.6 Conjugation frequency of clinical plasmids into MG1655 and MG1655Δ*sspB* +/- CRISPR plasmid

Due to problems with the donor strain for the mini-F plasmids, we performed conjugation experiments using clinical plasmids (from SK5384-5389 and SK3524 with pUUH239.2) with multiple resistance genes in order to test if the constructed CRISPR-Cas9 system is efficient in destroying genes that are conjugated into the cells. The results from the experiment in the MG1655 +/- CRISPR plasmid strains can be seen in Figure 12. There is no significant difference in conjugation frequency between the +CRISPR strain compared to the -CRISPR strain for any of the clinical plasmids. The most difference in conjugation frequency is observed for plasmid 5, however the error bar for the -CRISPR strain is considerably large in this case.

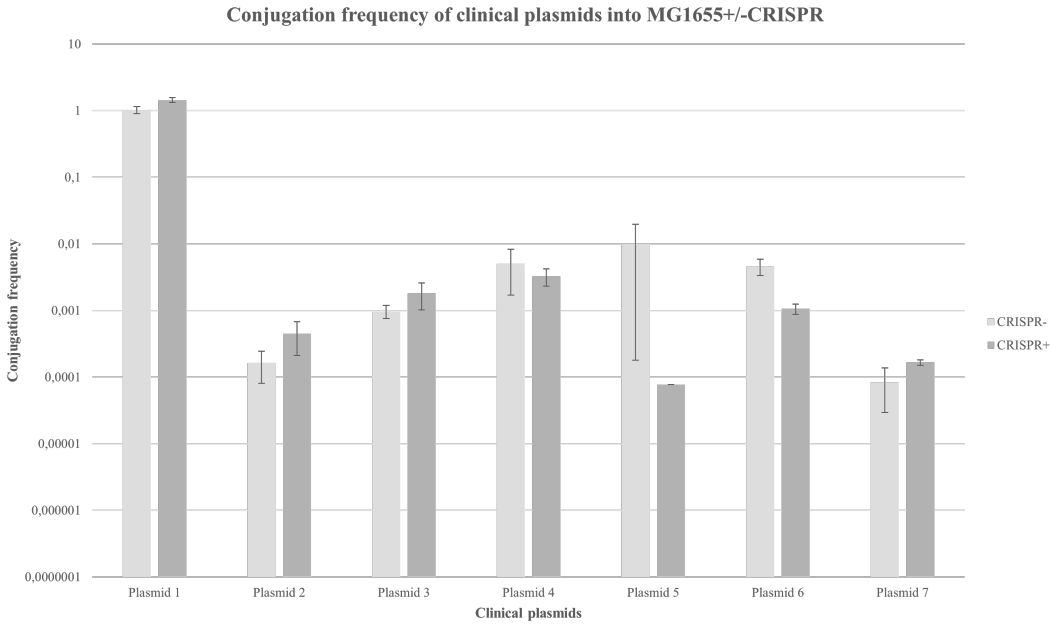

Figure 12: The figure presents the results from the conjugation assays with multiple resistance genes on clinical plasmids into MG1655 and MG1655 with the CRISPR plasmid. Plasmid number 7 is the pUUH239.2 plasmid. n = 3 (-CRISPR plasmid 4, 5, 6 and 7 , n=2 +CRISPR plasmid 5, n=1, +CRISPR plasmid 6 and 7, n=2 due to non-countable colonies).

The same clinical plasmids were conjugated into MG1655Δ*sspB* +/- CRISPR plasmid strains, see Figure 13. As observed in the wildtype experiment, no difference between the +/- strains was detected. The conjugation frequencies show similar values as in the wild type experiment and the increased level of Cas9 in the cells does not seem to play a role in the efficiency of the CRISPR-Cas9 system.

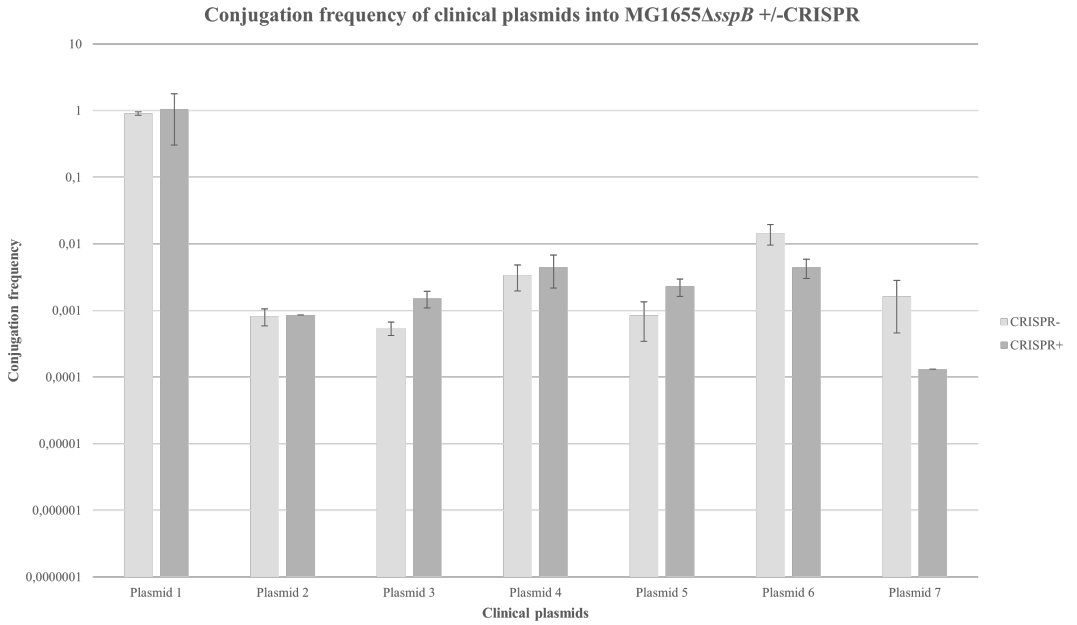

Figure 13: The figure presents the results from the conjugation assays with multiple resistance genes on clinical plasmids into MG1655ΔsspB and MG1655ΔsspB with the CRISPR plasmid. Plasmid number 7 is the pUUH239.2 plasmid. n = 3 (CRISPR- plasmid 4, 5, 6 and 7 , n=2 +CRISPR plasmid 5, n=1, +CRISPR plasmid 6 and 7, n=2 due to non-countable colonies).

The same experiments were performed using the *S. typhimurium* with the type I system consisting of the original CRISPR array. The results, seen in Figure A.11, are consistent with the results from the experiments with the CRISPR plasmid in MG1655 and MG1655Δ*sspB* (Figure 12 and 13). Collectively and surprisingly, the results from all conjugation assays indicate that the CRISPR-Cas9 system is not very efficient in destructing resistance genes when they enter the cells through conjugation.

5 Discussion

Here we show that CRISPR systems can be engineered to prevent HGT of antibiotic resistance genes. The protection provided varied between different spacers from 1000-fold for the *tetA* gene to 10-fold for *aac-(6')-Ib-cr*, when delivered by transformation. When spacers were delivered through transduction, protection varied between 100-fold for *tetA* to no effect for *dhfr*. Surprisingly, a significant difference in the transduction frequency between the CRISPR +/- strains was observed for *mph*, even though the CRISPR

array does not contain spacer sequences corresponding to *mph*. However, the *mrx* gene is commonly included with the *mphA-mrx-mphR* gene cluster and it is possible that the *mrx* gene is actually included in the SK5479 *mph* gene. To confirm whether or not this is the case, a sequencing of the construct should be performed.

Multiple unsuccessful attempts were made with lysates from the SK3786 strain containing *ctx-m-15*. It is uncertain if the fact that the SK3786 strain is a BW25113 strain and that the lysates of the SK3786 strains were prepared from MG1655 P1 lysate could affect the outcome of the experiment. A BW25113 P1 lysate could be used to repeat the experiment and see if that changes the outcome. Concludingly it could be worth building more constructs to test more resistance genes in order to see if the results are consistent with the transformation results.

To our surprise, presence of CRISPR-Cas9 did not prevent HGT of resistance genes through conjugation. Although lack of protection for one of the experiment could be accounted for by problems with the donor strains (SK5550 and SK5551) not being *dapA-*.To test DAP dependence and chloramphenicol resistance, the donor strains were plated on LA and cam selective plates. The fact that the donor strains showed growth on both plates suggests a mixed population where some cells are *dapA::cat* cassette and some are the wild type *dapA*. This means that the cfu on the LA+CEF/TP/TET plates in the conjugation experiments could potentially contain donor cells, resulting in an incorrectly calculated conjugation frequency. However, for the second experiment no such problems with the donor strain were observed. Yet, no difference in conjugation frequency of the clinical plasmids into the MG1655 and MG1655Δ*sspB* +/- CRISPR strains was observed. The clinical plasmids carry multiple resistance genes including *tetA* which the CRISPR system did confer protection against in the transformation and transduction experiments. This is surprising considering the fact that previous studies focusing on natural CRISPR systems have found indications of CRISPR provided protection against HGT via conjugation (Wheatley & MacLean 2021).

The lack of effect by the CRISPR system on conjugated resistance genes can have multiple explanations. DNA that enters cells through conjugation is single-stranded and is sequentially made double-stranded in the recipient cell (Llosa *et al.* 2002). CRISPR systems are designed to recognise foreign incoming DNA, however if the recognised DNA that enters the cell is single-stranded, Cas9 is not capable of cleaving the DNA due to the non-existing PAM. When the complementary strand has been synthesised it is possible that the system is not actively recognising the DNA as foreign anymore. In addition, it is possible that uptake through transformation and transduction induces a different kind of stress response in the cell that is important for the activation of the CRISPR-Cas9 system.

The clinical plasmid pUUH239.2 as well as the mini-F plasmid are low copy plasmids (Sandegren *et al.* 2012; Andrup & Andersen 1999) whereas the pBAD18 plasmid used for the transfer of resistance genes in the transformation experiments is a high copy number plasmid (https://novoprolabs.com/vector/Vgeytcmrw). It is difficult to conclude that the copy number of the plasmid affects the efficiency of the system, especially since conjugation and transformation presents contrasting mechanisms of transfer. To determine whether or not the copy number makes a difference, plasmids with different copy numbers would have to be tested in the conjugation and transformation experiments respectively.

An additional consideration of the conjugation experiments is that the clinical plasmid as well as the mini-F plasmids demonstrated a high conjugation frequency. Andrup Andersen (1999) determined that the number of *E. coli* transconjugants receiving F plasmids was 0.15 per donor per minute. If the rate of transfer would be lower, would the CRISPR-Cas9 system confer more protection against resistance genes? More plasmids would have to be tested in order to determine if the conjugation rate and frequency affects the performance of the CRISPR-Cas9 system.

Our initial experiments did not show great protection by the engineered CRISPR system against HGT of resistance genes. A possible reason was that we added a SsrA degradation tag to the Cas9 protein in our design to ensure that Cas9 levels in the cells would not become too high due to the strong constitutive J23101 promoter (https://parts.igem.org/Part:BBa_J23101). The SspB protein binds to the ssrA degradation tag consequently promoting degradation by proteases (Farrell *et al.* 2005). Farell *et al.* (2005) determined that wild-type levels of SspB does not induce complete degradation of ssrA tagged proteins with a strong synthetic constitutive promoter (CP25), yet deletion of *sspB* in cells should stabilize any protein with an ssrA tag. Deletion of *sspB* showed an increased protection against HGT mediated by transduction and transformation, suggesting that the amount of Cas9 in the cells is important for the efficiency of the CRISPR-Cas9 system. The results from the western blot did indicate a small difference in the level of Cas9 between the MG1655 and MG1655Δ*sspB* strains. Repeting the western blot experiment with quantification would be valuable in order to conclude how Cas9 levels affect protection against HGT. Furthermore, the binding between target and antibody exhibits a narrow range of linearity, where the semi-logarithmic binding curve contains two plateaus for concentrations outside the linear range (Suzuki *et al.* 2011). It is possible that for some of the samples, the amount of Cas9, or RpoB lies outside the linear range of the binding to the antibody. For more precise quantification, a standard curve using different predetermined concentrations of Cas9 should be constructed. In this way, the dynamic range of the western blot can be characterised and can then be used to directly translate mean gray values to concentrations of Cas9.

As seen in Figure 7, the TSS-treated sample contained lower levels of Cas9 in the cells compared to the non-treated samples. The TSS buffer contains the regular components in LB media and additional $MgCl_2 \cdot 6H_2O$, DMSO and PEG3350 additives (Chung *et al.* 1989). PEG3350 and the cations in $MgCl_2$ promote uptake of foreign DNA and thereby generate competent cells (Chung *et al.* 1989). The lower levels of Cas9 in the TSS-treated cells could indicate that some form of stress response, making them competent also results in increased degradation of some proteins. A difference in size of the Cas9 proteins was observed when comparing the non-treated samples to the TSS-treated samples in Figure 7. The fact that the same size difference can be observed for the reference protein in Figure 8 indicates that there is something in the TSS buffer that changes the folding of the protein. If this affects the nuclease activity of Cas9 could be tested by transforming the same plasmids into the cells through e.g., electroporation.

In addition to the western blot experiment, the transcription levels of tracr RNA and the *cas9* gene , but not the CRISPR array were intended to be monitored through RT-qPCR. The palindromic repeats in the CRISPR array complicate the amplification as the mRNA creates a secondary structure consisting of hairpin formations, making monitoring of the CRISPR repeats difficult. However, the CRISPR array and the *cas9* gene were designed to be transcribed from the same pJ23101 promoter, so monitoring of cas9 levels should be adequate for determining the expression level of the CRISPR array. The tracr sequence is expressed under its native promoter and the exact expression levels and regulatory conditions are unknown. However, a failed RNA preparation prevented the finalisation of the experiment due to time constraints and only a calibration curve was created. The RT-qPCR would have been a useful experiment, giving insights in the levels of tracr in the cells and whether or not the levels of tracr are sufficient could have been examined.

In conclusion, the protection provided by the engineered CRISPR system seems most powerful against HGT through transformation and seems to be affected by the levels of Cas9 in the targeted cell, although the latter requires further experimental investigation. The spacer corresponding to the *tetA* gene was most efficient, resulting in the highest difference in resistance gene transfer between the +/- CRISPR strains. Why this spacer was much more effective than others is interesting and should be investigated more by bioinformatic analyses, but an interesting observation is that this spacer is the first spacer in the array. Thus, it is possible that the expression level of this spacer is higher than that of the remaining spacers and this is why it is most effective. However, the *oxa-1* spacer which has no protective effect at all, is the second spacer so the order of spacers can not explain all the differences observed. Overall, we conclude that the CRISPR-Cas9 system can actively protect probiotic strains against resistance genes obtained through horizontal gene transfer, but that the design of the construct as well as the conditions and mechanisms of transfer need to be investigated further.

6 Acknowledgements

Firstly, I would like to thank my supervisor Sanna Koskiniemi for introducing this project to me and guiding me throughout the whole process. I have learned a lot listening to the impressing and important research performed in your group.

Secondly I would like to to thank my subject reader Linus Sandegren for your guidance as well as providing constructs and strains to my project.

An additional thank you to Danna Lee for teaching me all your inventive tips and tricks in the lab and giving valuable inputs to the project.

To all the people in SK Lab, thank you for being welcoming and always helping me out in the lab.

References

Andrup L, Andersen K. 1999. A comparison of the kinetics of plasmid transfer in the conjugation systems encoded by the F plasmid from Escherichia coli and plasmid pCF10 from Enterococcus faecalis. Microbiology 145: 2001–2009. Publisher: Microbiology Society,.

Antunes P, Machado J, Sousa JC, Peixe L. 2005. Dissemination of Sulfonamide Resistance Genes (sul1, sul2, and sul3) in Portuguese Salmonella enterica Strains and Relation with Integrons. Antimicrobial Agents and Chemotherapy 49: 836–839.

Becker B, Cooper MA. 2013. Aminoglycoside antibiotics in the 21st century. ACS chemical biology 8: 105–115.

Bello-López JM, Cabrero-Martínez OA, Ibáñez-Cervantes G, Hernández-Cortez C, Pelcastre-Rodríguez LI, Gonzalez-Avila LU, Castro-Escarpulli G. 2019. Horizontal Gene Transfer and Its Association with Antibiotic Resistance in the Genus Aeromonas spp. Microorganisms 7: 363.

Bethel CR, Distler AM, Ruszczycky MW, Carey MP, Carey PR, Hujer AM, Taracila M, Helfand MS, Thomson JM, Kalp M, Anderson VE, Leonard DA, Hujer KM, Abe T, Venkatesan AM, Mansour TS, Bonomo RA. 2008. Inhibition of OXA-1 beta-lactamase by penems. Antimicrobial Agents and Chemotherapy 52: 3135–3143.

Cabezón E, Ripoll-Rozada J, Peña A, de la Cruz F, Arechaga I. 2015. Towards an integrated model of bacterial conjugation. FEMS microbiology reviews 39: 81–95.

Chopra I, Roberts M. 2001. Tetracycline Antibiotics: Mode of Action, Applications, Molecular Biology, and Epidemiology of Bacterial Resistance. Microbiology and Molecular Biology Reviews 65: 232–260.

Chung CT, Niemela SL, Miller RH. 1989. One-step preparation of competent Escherichia coli: transformation and storage of bacterial cells in the same solution. Proceedings of the National Academy of Sciences 86: 2172–2175.

Correia S, Poeta P, Hébraud M, Capelo JL, Igrejas G. 2017. Mechanisms of quinolone action and resistance: where do we stand? Journal of Medical Microbiology 66: 551–559.

de Castro Spadari C, Vila T, de Morais Barroso V, Ishida K. 2021. New targets for the development of antifungal agents. Óscar Zaragoza, Casadevall A, editors, Encyclopedia of Mycology, Elsevier, Oxford, 456–467.

Dedeic-Ljubovic A, Hukic M, Pfeifer Y, Witte W, Padilla E, López-Ramis I, Albertí S. 2010. Emergence of CTX-M-15 extended-spectrum β-lactamase-producing Klebsiella pneumoniae isolates in Bosnia and Herzegovina. Clinical Microbiology and Infection 16: 152–156.

Farah Y, Oussama M, Jehad H. 2018. Sulfonamides: Historical Discovery Development (Structure-Activity Relationship Notes). In-vitro In-vivo In-silico Journal 1: 1 – 15.

Farrell CM, Grossman AD, Sauer RT. 2005. Cytoplasmic degradation of ssrA-tagged proteins. Molecular Microbiology 57: 1750–1761.

Frasson I, Cavallaro A, Bergo C, Richter SN, Palù G. 2011. Prevalence of aac(6')-Ib-cr plasmid-mediated and chromosome-encoded fluoroquinolone resistance in Enterobacteriaceae in Italy. Gut Pathogens 3: 12.

Griffiths AJ, Miller JH, Suzuki DT, Lewontin RC, Gelbart WM. 2000. Transduction. An Introduction to Genetic Analysis. 7th edition Publisher: W. H. Freeman.

Gupta D, Bhattacharjee O, Mandal D, Sen MK, Dey D, Dasgupta A, Kazi TA, Gupta R, Sinharoy S, Acharya K, Chattopadhyay D, Ravichandiran V, Roy S, Ghosh D. 2019. CRISPR-Cas9 system: A new-fangled dawn in gene editing. Life Sciences 232: 116636.

Heikkilä E, Skurnik M, Sundström L, Huovinen P. 1993. A novel dihydrofolate reductase cassette inserted in an integron borne on a Tn21-like element. Antimicrobial Agents and Chemotherapy 37: 1297–1304.

Hussein AIA, Ahmed AM, Sato M, Shimamoto T. 2009. Characterization of integrons and antimicrobial resistance genes in clinical isolates of Gram-negative bacteria from Palestinian hospitals. Microbiology and Immunology 53: 595–602. _eprint: https://onlinelibrary.wiley.com/doi/pdf/10.1111/j.1348-0421.2009.00168.x.

Hutchings MI, Truman AW, Wilkinson B. 2019. Antibiotics: past, present and future. Current Opinion in Microbiology 51: 72–80.

Irrgang A, Falgenhauer L, Fischer J, Ghosh H, Guiral E, Guerra B, Schmoger S, Imirzalioglu C, Chakraborty T, Hammerl JA, Käsbohrer A. 2017. CTX-M-15-Producing E. coli Isolates from Food Products in Germany Are Mainly Associated with an IncF-Type Plasmid and Belong to Two Predominant Clonal E. coli Lineages. Frontiers in Microbiology 8: 2318.

Isgren CM, Edwards T, Pinchbeck GL, Winward E, Adams ER, Norton P, Timofte D, Maddox TW, Clegg PD, Williams NJ. 2019. Emergence of carriage of CTX-M-15 in faecal Escherichia coli in horses at an equine hospital in the UK; increasing prevalence over a decade (2008–2017). BMC Veterinary Research 15: 268.

Jiang H, Cheng H, Liang Y, Yu S, Yu T, Fang J, Zhu C. 2019. Diverse Mobile Genetic Elements and Conjugal Transferability of Sulfonamide Resistance Genes (sul1, sul2, and sul3) in Escherichia coli Isolates From Penaeus vannamei and Pork From Large Markets in Zhejiang, China. Frontiers in Microbiology 10: 1787.

Jiang F, Doudna JA. 2017. CRISPR–Cas9 Structures and Mechanisms. Annual Review of Biophysics 46: 505–529. _eprint: https://doi.org/10.1146/annurev-biophys-062215-010822.

Johnston C, Martin B, Fichant G, Polard P, Claverys JP. 2014. Bacterial transformation: distribution, shared mechanisms and divergent control. Nature Reviews Microbiology 12: 181–196. Bandiera_abtest: a Cg_type: Nature Research Journals Number: 3 Primary_atype: Reviews Publisher: Nature Publishing Group Subject_term: Bacterial genetics;Bacterial transformation;Cellular microbiology Subject_term_id: bacterial-genetics;bacterial-transformation;cellular-microbiology.

June CM, Vallier BC, Bonomo RA, Leonard DA, Powers RA. 2014. Structural Origins of Oxacillinase Specificity in Class D β-Lactamases. Antimicrob Agents Chemother 58: 333–341.

Kalkut G. 1998. Sulfonamides and trimethoprim. Cancer Investigation 16: 612–615.

de Kraker MEA, Stewardson AJ, Harbarth S. 2016. Will 10 Million People Die a Year due to Antimicrobial Resistance by 2050? PLOS Medicine 13: 1–6. Publisher: Public Library of Science.

Lenz KD, Klosterman KE, Mukundan H, Kubicek-Sutherland JZ. 2021. Macrolides: From Toxins to Therapeutics. Toxins 13: 347. Number: 5 Publisher: Multidisciplinary Digital Publishing Institute.

Lerminiaux NA, Cameron AD, *. 2019. Horizontal transfer of antibiotic resistance genes in clinical environments. Canadian Journal of Microbiology 65: 34–44. Publisher: NRC Research Press.

Liu YY, Wang Y, Walsh TR, Yi LX, Zhang R, Spencer J, Doi Y, Tian G, Dong B, Huang X, Yu LF, Gu D, Ren H, Chen X, Lv L, He D, Zhou H, Liang Z, Liu JH, Shen J. 2016. Emergence of plasmid-mediated colistin resistance mechanism MCR-1 in animals and human beings in China: a microbiological and molecular biological study. The Lancet. Infectious Diseases 16: 161–168.

Livermore DM, Day M, Cleary P, Hopkins KL, Toleman MA, Wareham DW, Wiuff C, Doumith M, Woodford N. 2019. OXA-1 β-lactamase and non-susceptibility to penicillin/β-lactamase inhibitor combinations among ESBL-producing Escherichia coli. Journal of Antimicrobial Chemotherapy 74: 326–333.

Llosa M, Gomis-Rüth FX, Coll M, de la Cruz Fd F. 2002. Bacterial conjugation: a two-step mechanism for DNA transport. Molecular Microbiology 45: 1–8.

Makarova KS, Wolf YI, Koonin EV. 2013. Comparative genomics of defense systems in archaea and bacteria. Nucleic Acids Research 41: 4360–4377.

Michael GB, Cardoso M, Schwarz S. 2005. Identification of an aadA2 gene cassette from Salmonella enterica subsp. enterica Serovar derby. Journal of Veterinary Medicine. B, Infectious Diseases and Veterinary Public Health 52: 456–459.

Møller TSB, Overgaard M, Nielsen SS, Bortolaia V, Sommer MOA, Guardabassi L, Olsen JE. 2016. Relation between tetR and tetA expression in tetracycline resistant Escherichia coli. BMC Microbiology 16: 39.

Muthukrishnan AB, Kandhavelu M, Lloyd-Price J, Kudasov F, Chowdhury S, Yli-Harja O, Ribeiro AS. 2012. Dynamics of transcription driven by the tetA promoter, one event at a time, in live Escherichia coli cells. Nucleic Acids Research 40: 8472–8483.

Myers AG, Clark RB. 2021. Discovery of Macrolide Antibiotics Effective against Multi-Drug Resistant Gram-Negative Pathogens. Acc Chem Res 54: 1635–1645.

Ogbolu DO, Alli OAT, Webber MA, Oluremi AS, Oloyede OM. 2018. CTX-M-15 is Established in Most Multidrug-Resistant Uropathogenic Enterobacteriaceae and Pseudomonaceae from Hospitals in Nigeria. European Journal of Microbiology & Immunology 8: 20–24.

Park CH, Robicsek A, Jacoby GA, Sahm D, Hooper DC. 2006. Prevalence in the United States of *aac(6′)-Ib-cr* Encoding a Ciprofloxacin-Modifying Enzyme. Antimicrobial Agents and Chemotherapy 50: 3953–3955. _eprint: https://journals.asm.org/doi/pdf/10.1128/AAC.00915-06.

Paterson DL, Bonomo RA. 2005. Extended-Spectrum β-Lactamases: a Clinical Update. Clinical Microbiology Reviews 18: 657–686.

Pham TDM, Ziora ZM, Blaskovich MAT. 2019. Quinolone antibiotics. MedChemComm 10: 1719–1739.

Poirel L, Gerome P, De Champs C, Stephanazzi J, Naas T, Nordmann P. 2002. Integron-Located oxa-32 Gene Cassette Encoding an Extended-Spectrum Variant of OXA-2 β-Lactamase from Pseudomonas aeruginosa. Antimicrob Agents Chemother 46: 566–569.

Poole TL, Callaway TR, Bischoff KM, Warnes CE, Nisbet DJ. 2006. Macrolide inactivation gene cluster mphA-mrx-mphR adjacent to a class 1 integron in Aeromonas

hydrophila isolated from a diarrhoeic pig in Oklahoma. The Journal of Antimicrobial Chemotherapy 57: 31–38.

Riquelme NA, Leon MF, Santander JA, Robeson JP. 2019. Productive infection and transduction by bacteriophage P1 in the species Salmonella bongori. Electronic Journal of Biotechnology 41: 9–12.

Sandegren L, Linkevicius M, Lytsy B, Melhus Å, Andersson DI. 2012. Transfer of an Escherichia coli ST131 multiresistance cassette has created a Klebsiella pneumoniae-specific plasmid associated with a major nosocomial outbreak. The Journal of Antimicrobial Chemotherapy 67: 74–83.

Scholar E. 2007. Sulfonamides. Enna SJ, Bylund DB, editors, xPharm: The Comprehensive Pharmacology Reference, Elsevier, New York, 1–4.

Singh SB, Young K, Silver LL. 2017. What is an "ideal" antibiotic? Discovery challenges and path forward. Biochemical Pharmacology 133: 63–73.

Starosta AL, Karpenko VV, Shishkina AV, Mikolajka A, Sumbatyan NV, Schluenzen F, Korshunova GA, Bogdanov AA, Wilson DN. 2010. Interplay between the Ribosomal Tunnel, Nascent Chain, and Macrolides Influences Drug Inhibition. Chemistry & Biology 17: 504–514.

Suzuki O, Koura M, Noguchi Y, Uchio-Yamada K, Matsuda J. 2011. Use of sample mixtures for standard curve creation in quantitative western blots. Experimental Animals 60: 193–196.

Tacic A, Nikolic V, Nikolic L, Savic I. 2017. Antimicrobial sulfonamide drugs. Advanced technologies 6: 58–71.

Tadesse DA, Zhao S, Tong E, Ayers S, Singh A, Bartholomew MJ, McDermott PF. 2012. Antimicrobial Drug Resistance in Escherichia coli from Humans and Food Animals, United States, 1950–2002. Emerging Infectious Diseases 18: 741–749.

Tooke CL, Hinchliffe P, Bragginton EC, Colenso CK, Hirvonen VHA, Takebayashi Y, Spencer J. 2019. β-Lactamases and β-Lactamase Inhibitors in the 21st Century. Journal of Molecular Biology 431: 3472–3500.

Tumuluri VS, Rajgor V, Xu SY, Chouhan OP, Saikrishnan K. 2021. Mechanism of DNA cleavage by the endonuclease SauUSI: a major barrier to horizontal gene transfer and antibiotic resistance in Staphylococcus aureus. Nucleic Acids Research 49: 2161–2178.

Virtanen P, Wäneskog M, Koskiniemi S. 2019. Class II contact-dependent growth inhibition (CDI) systems allow for broad-range cross-species toxin delivery within the Enterobacteriaceae family. Molecular Microbiology 111: 1109–1125.

Wheatley RM, MacLean RC. 2021. CRISPR-Cas systems restrict horizontal gene transfer in Pseudomonas aeruginosa. ISME J 15: 1420–1433. Bandiera_abtest: a Cc_license_type: cc_by Cg_type: Nature Research Journals Number: 5 Primary_atype: Research Publisher: Nature Publishing Group Subject_term: Evolution;Microbial genetics;Microbiology Subject_term_id: evolution;microbial-genetics;microbiology.

WHO. 2019. New report calls for urgent action to avert antimicrobial resistance crisis. https://www.who.int/news/item/29-04-2019-new-report-calls-for-urgent-action-to-avert-antimicrobial-resistance-crisis. Retrieved 2021-10-01.

Wróbel A, Arciszewska K, Maliszewski D, Drozdowska D. 2020. Trimethoprim and other nonclassical antifolates an excellent template for searching modifications of dihydrofolate reductase enzyme inhibitors. The Journal of Antibiotics 73: 5–27.

Yoshida N, Sato M. 2009. Plasmid uptake by bacteria: a comparison of methods and efficiencies. Applied Microbiology and Biotechnology 83: 791–798. Company: Springer Distributor: Springer Institution: Springer Label: Springer Number: 5 Publisher: Springer Berlin Heidelberg.

Zinner SH. 2007. Antibiotic use: present and future 5.

A Appendices

A.1 Cloning of the pWEB-TNC::tracr-cas9-CRISPR plasmid

A.1.1 Transformation protocol

All transformations during the cloning of the pWEB-TNC::tracr-cas9-CRISPR plasmid were made using NEB® 5-alpha Competent *E. coli*. The cells were thawed on ice for 10 mins and 10-25 µl of cells were transferred to an eppendorf for each transformation. 1-2.5 µl of ligation mix was added to the cell mixture and the tube was flicked 4-5 times. The mixture was kept on ice for 30 minutes and heat-shocked for 30 s at 42 °C. The cells were kept on ice for 5 minutes and 500 µl of SOC medium was added. The cells were recovered at 37 °C at 200 rpm for 60 minutes. LA ampicillin plates were used for selection of transformed cells throughout the cloning of the pWEB-TNC::tracr-cas9-CRISPR plasmid. The selective plates were incubated for 16-18 hours at 37°C. The concentration of the plasmid preparation of the final pWEB-TNC::tracr-cas9-CRISPR construct was measured to 226.6 ng/µl.

A.1.2 PCR and cloning conditions

Table A1: The table presents the set up for one Taq colony PCR reaction

List of strains		
Name	**Description**	**Antibiotic resistance**
10X	DreamTaq buffer	2
10 mM	dNTPs	0.4
10 µ	F primer	2
10 µ	R primer	2
5 U/µl	DreamTaq	0.2
	H_2O	13.4
	Total volume	20

Table A2: Phusion PCR reaction set up (one reaction)

	Volume (µl)
5X Phusion HF buffer	4
dNTPs	0.4
F primer	1
R primer	1
Phusion Polymerase	0.1
DNA	1 ul
H_2O	12.5
Total volume	20

Table A3: Digestion of 500 ng pWEB-TNC plasmid

	Volume (µl)
DNA	2.8
FastDigest buffer	2
FastDigest SmaI	1
FastDigest HindlII	1
FastAP	1
H_2O	12.7
Total volume	20

Table A4: Alignment of linker oligos

Temperature (°C)	Time (min)
98	2
95	5
90	5
85	5
75	5
70	5
65	5
60	5
55	5
50	5
45	5
40	5
35	5
30	5
25	5
20	forever

Table A5: The table presents the ligation reaction for the digested pWEB-TNC plasmid and the aligned linker sequence

Ligation of pWEB-TNC and linker			
	1:10 dilution	**1:100 dilution**	**1:10000 dilution**
30 ng vector	2	2	2
Diluted linker	1	1	1
T4 DNA ligase buffer	1	1	1
T4 DNA ligase	1	1	1
H_2O	5	5	5
Total volume (μl)	10		

Table A6: Screening of linker

Temperature (°C)	Time (min)
1x	
95	2
30x	
95	0.5
58	0.5
72	1
1x	
72	2

Table A7: The table presents the digestion reaction to screen for the linker sequence

Test digest of pWEB-TNC::linker with SalI and PstI		
Name	**Control (pWEB-TNC)**	**pWEB-TNC::linker (μl)**
300 ng DNA	1.7	1.6
FastDigest buffer	1	1
FastDigest SalI	0.5	0.5
FastDigest PstI	0.5	0.5
H_2O	6.3	6.4
	Total volume (μl)	10

Table A8: PCR program for amplification of tracr and cas9 genes

Temperature (°C)	Time (min)
1x	
98	5
35x	
98	0.5
65	0.5
72	2.5
1x	
72	5

Table A9: The table presents the Phusion PCR reaction to amplify the Cas9 gene from different templates

Phusion PCR of Cas9				
Name	**Colony**	**Nested PCR**	**Plasmid**	**Control**
Template	colony	2	0.2	colony
5X Phusion HF buffer	10	10	10	10
10 mM dNTPs	1	1	1	1
10 µlM F primer	2.5	2.5	2.5	2.5
10 µlM R primer	2.5	2.5	2.5	2.5
50 mM MgC_2	0.5	0.5	0.5	0.5
Phusion polymerase	0.5	0.5	0.5	0.5
H_2O	33	31	32.8	33
Total volume (µl)		50		

Table A10: The digestion reaction to prepare pWEB-TNC::linker, tracr and Cas9 for ligation

Digestion reaction			
	pWEB-TNC::linker	**Cas9**	**tracr**
DNA	10	21	18
FastDigest buffer	4	4	4
FD enzyme 1	2 (SmaI)	2 (SalI)	0.5 (SmaI)
FD enzyme 2	2 (BglII)	2 (BglII)	0.5 (SalI)
1 FastAP	1		
H_2O	21	11	17
Total volume (μl)		40	

Table A11: The ligation reaction of pWEB-TNC::linker, tracr and Cas9

Ligation reaction		
	pWEB-TNC::linker+cas9+tracr	
50 ng vector	1.4	
Cas9	2.8	
tracr	4.4	
T4 DNA ligase buffer	1.5	
T4 DNA ligase	1	
H_2O	3.9	
Total volume (μl)		15

Table A12: The digestion reaction to prepare pWEB-TNC::tracr-Cas9 and CRISPR vector for ligation

	Digestion reaction	
	pWEB-TNC::tracr-cas9	**CRISPR vector**
DNA	6.6	13.6
FastDigest buffer	4	4
FD XhoI	2	2
FD BglII	2	2
1 FastAP	1	
H_2O	24.4	18.4
Total volume (μl)		40

Table A13: The ligation reaction of pWEB-TNC::tracr-Cas9 and CRISPR array

	Ligation reaction	
	pWEB-TNC::linker::tracr-cas9+CRISPR array	
50 ng vector	3.1	
CRISPR insert	0.5	
T4 DNA ligase buffer	1	
T4 DNA ligase	1	
H_2O	4.4	
Total volume (μl)		10

A.1.3 Agarose gel images from the construction of the CRISPR plasmid

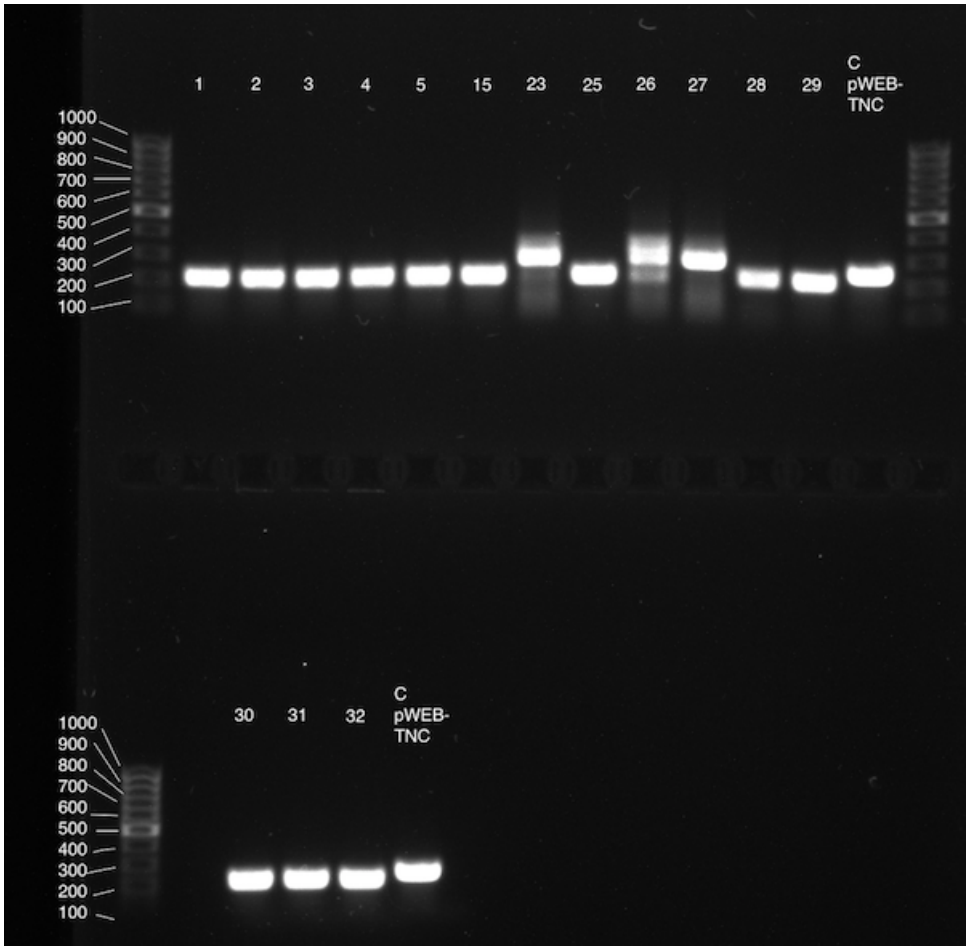

Figure A.1: Screening pWEB-TNC::linker for the linker sequence using oligos SK1926 and SK1927. The expected size difference between pWEB-TNC and pWEB-TNC::linker is 37 bp. Number 32 shows a smaller size than the control pWEB-TNC plasmid and was used in the following cloning steps. Ladder: Thermo Scientific™ GeneRuler 1 kb DNA Ladder.

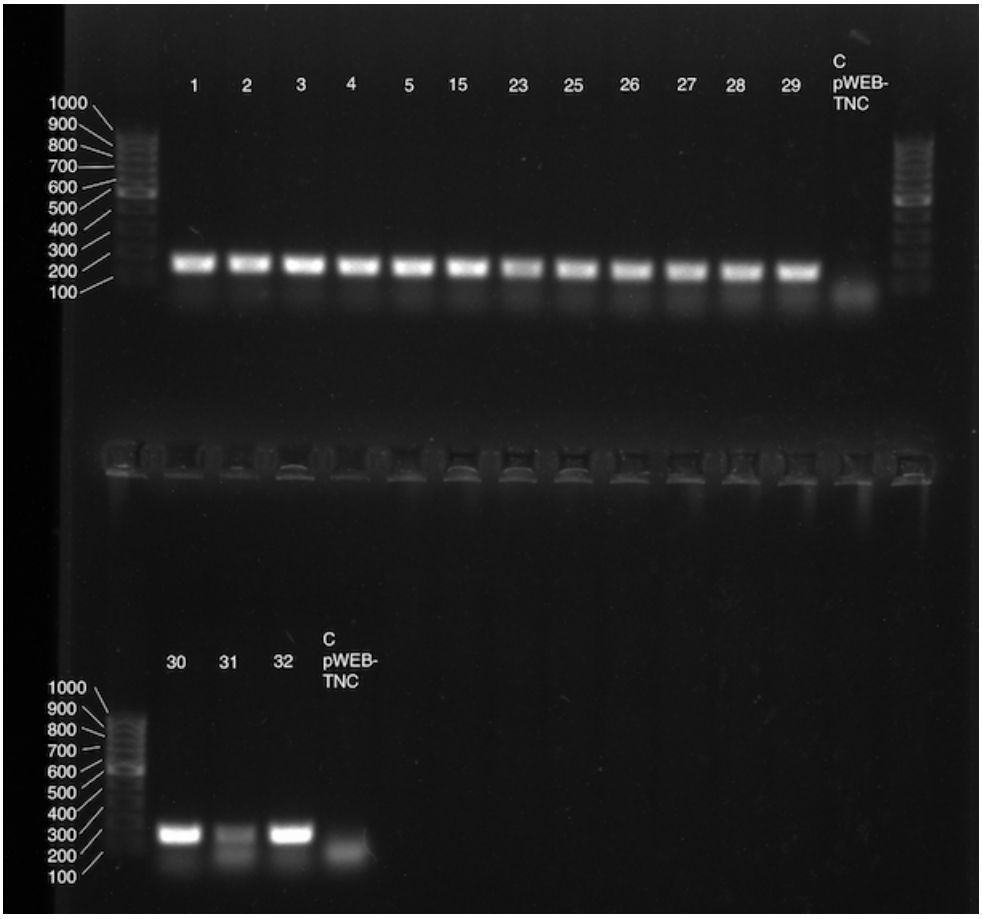

Figure A.2: Screening pWEB-TNC::linker for the linker sequence using oligos SK1926 and SK1985 (binding on the linker sequence). The expected size of the pWEB-TNC::linker amplification is 157 bp. Number 32 shows a band of the expected size and was used in the sequential cloning step. The negative control contained the pWEB-TNC::linker product and the ladder used was Thermo Scientific™ GeneRuler 100 bp DNA Ladder.

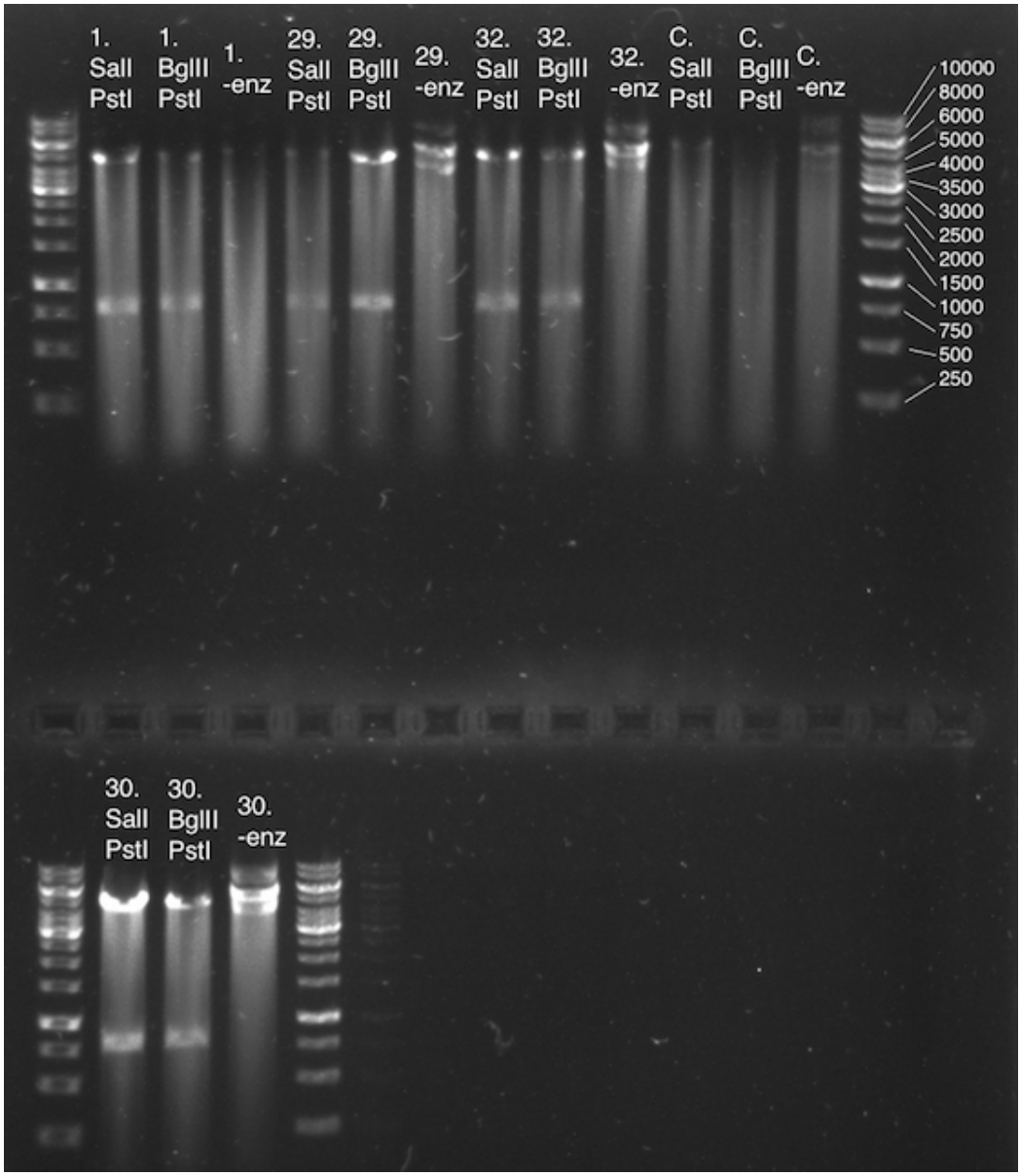

Figure A.3: Test digest of pWEB-TNC::linker using PstI and BglII as well as PstI and SalI restriction enzymes. The expected sizes of the pWEB-TNC::linker PstI and BglII digest fragments are 816 and 4959 bp. The expected sizes with PstI and SalI are 799 and 4976 bp. Number 32 shows two bands of the expected sizes and was used in the sequential cloning step. The negative controls contained no enzyme and the ladder used was Thermo Scientific™ GeneRuler 1 kb DNA Ladder.

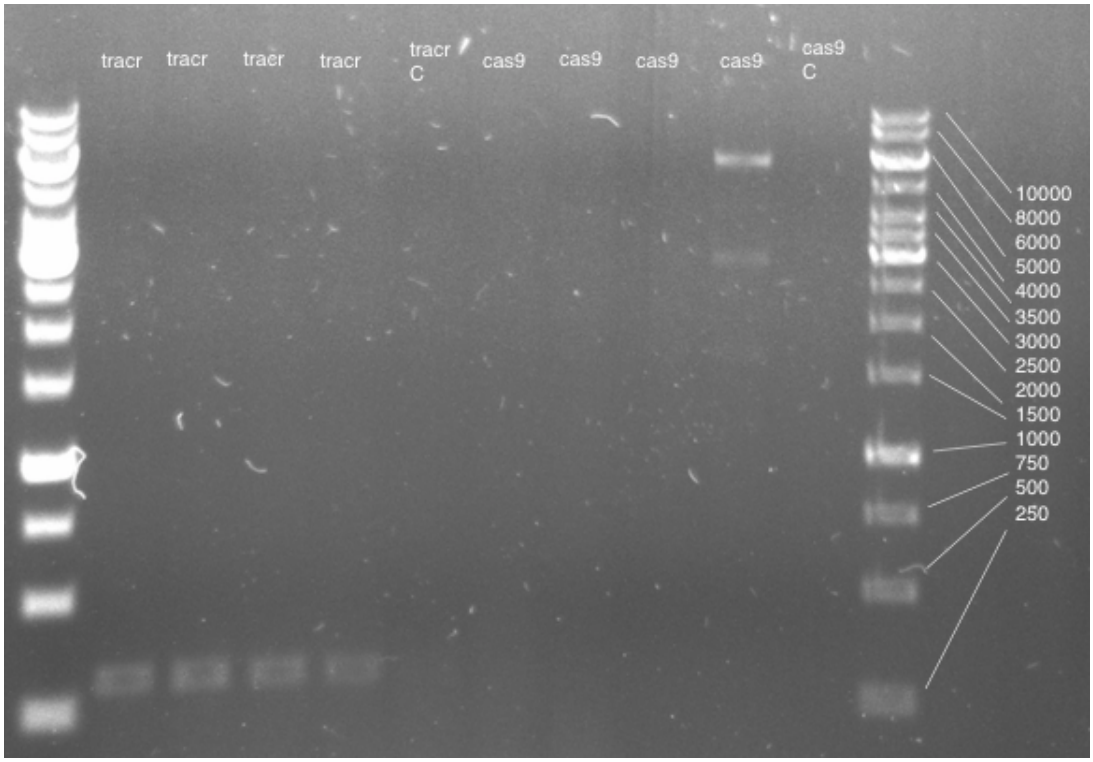

Figure A.4: The image shows an agarose gel of the tracr and Cas9 sequences that were amplified using Phusion PCR. Primers SK1805 and SK1806 were used for the amplification of tracr and SK1807 and SK1808 were used for the amplification of Cas9. The four tracr PCR products showed the expected size of 291 bp. No bands of the correct size were visible for the Cas9 products. The negative controls contained no template and the ladder used was Thermo Scientific™ GeneRuler 1 kb DNA Ladder.

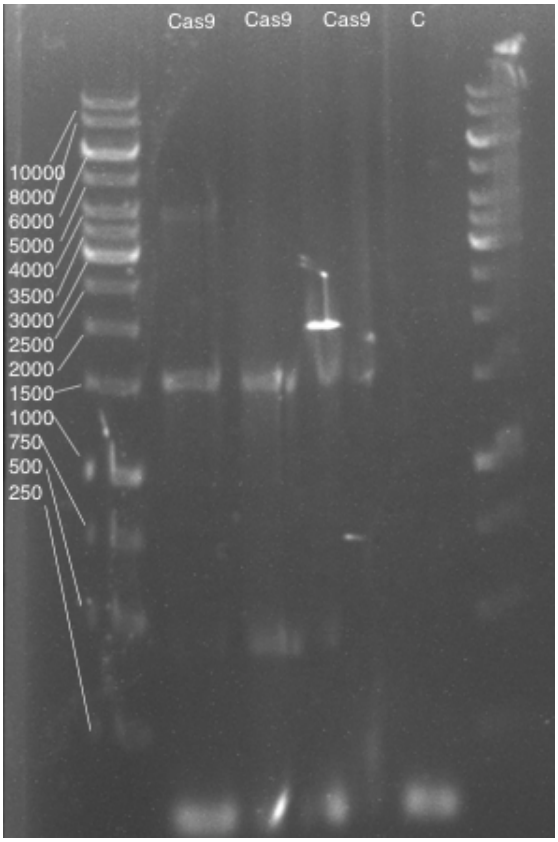

Figure A.5: The image shows an agarose gel of Cas9 sequences that were amplified using Phusion PCR. Primers SK1807 and SK1808 were used for the amplification. The first lane shows a faint band around the expected size of 4164 bp. The negative control contained no template and the ladder used was Thermo Scientific™ GeneRuler 1 kb DNA Ladder.

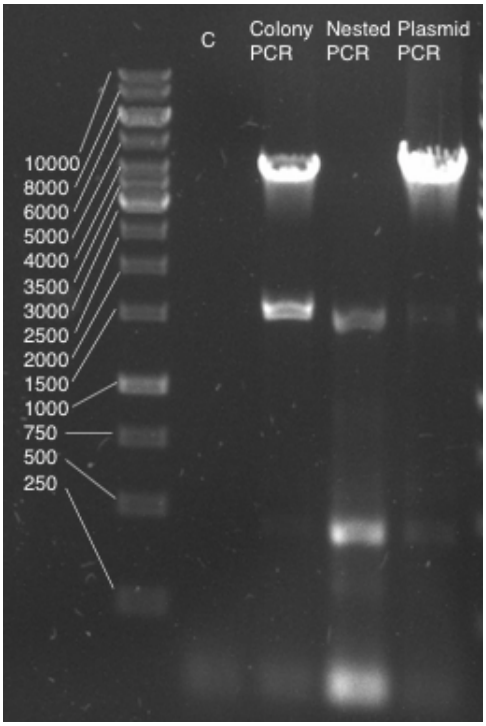

Figure A.6: The image shows the agarose gel of the pJ23101-cas9-deg products that were amplified using Phusion PCR. One colony PCR, one nested PCR and one PCR from SK4768 plasmid template were performed. The colony PCR and the plasmid PCR showed bands around the expected size of 4696 bp. The negative control contained no template and the ladder used was Thermo Scientific™ GeneRuler 1 kb DNA Ladder.

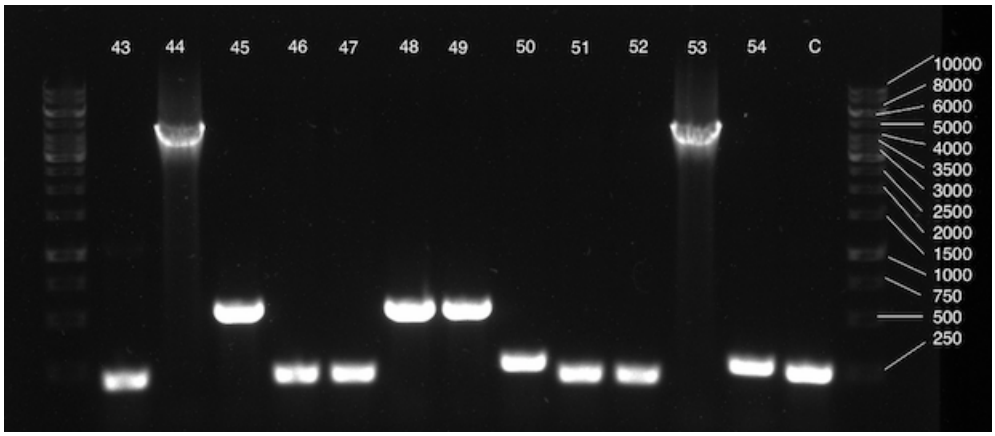

Figure A.7: The image shows the agarose gel of the screening of the tracr-pJ23101-cas9-deg products that were amplified using Taq PCR with primers SK1926 and SK1927. Products number 44 and 53 show bands around the expected size of 4696 bp. The control contained the pWEB-TNC::linker product with an expected size of 219 bp and the ladder used was Thermo Scientific™ GeneRuler 1 kb DNA Ladder.

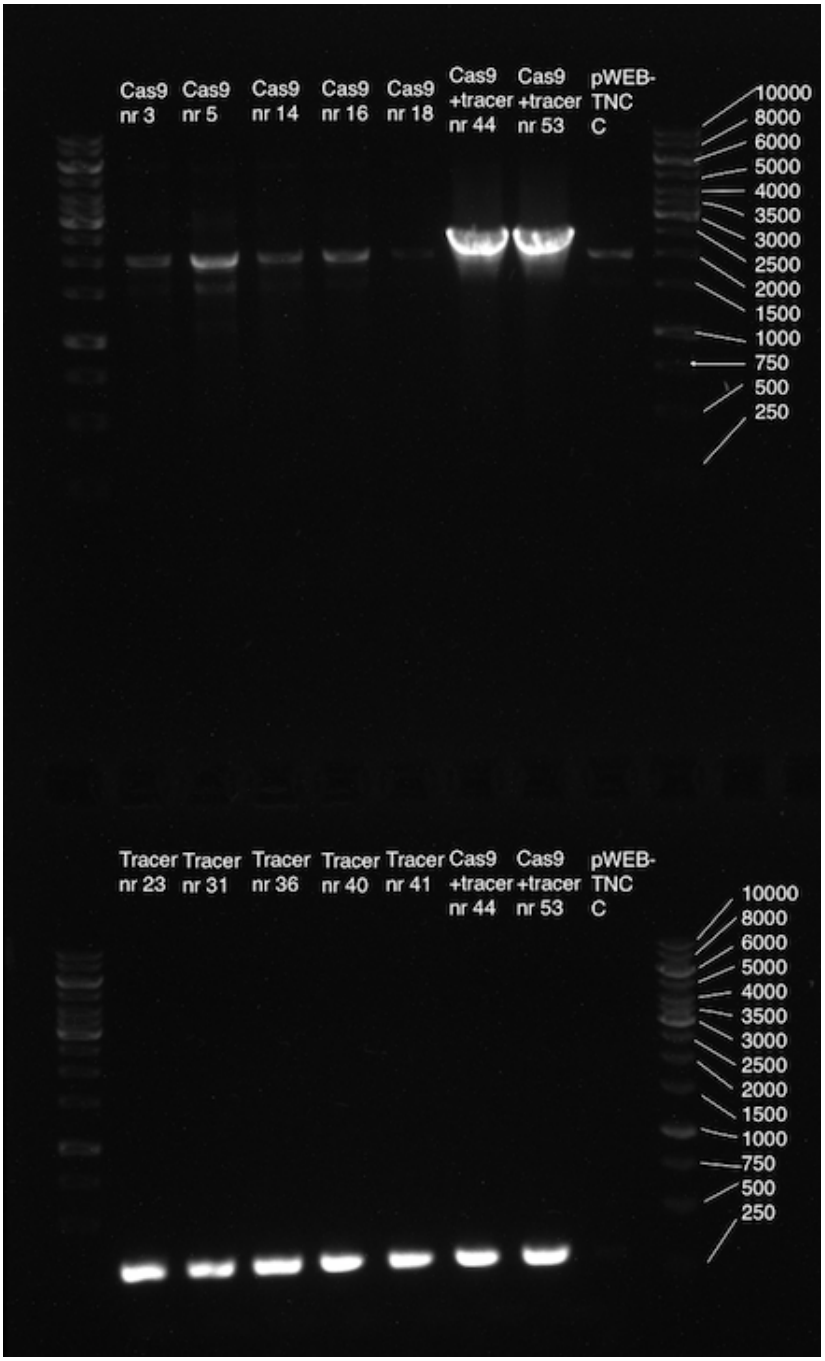

Figure A.8: The image shows the agarose gel of the screening of the tracr-pJ23101-cas9-deg products that were amplified using Taq PCR. The Cas9 sequence was screened with primers SK1926 and SK1929 and the tracr sequence was screened with primers SK1930 and SK1931. Product number 44 shows a band around the expected size of 2664 bp and 318 bp for the Cas9 and tracr sequences respectively and was used in the sequential cloning step. The negative control contained the pWEB-TNC::linker product and the ladder used was Thermo Scientific™ GeneRuler 1 kb DNA Ladder.

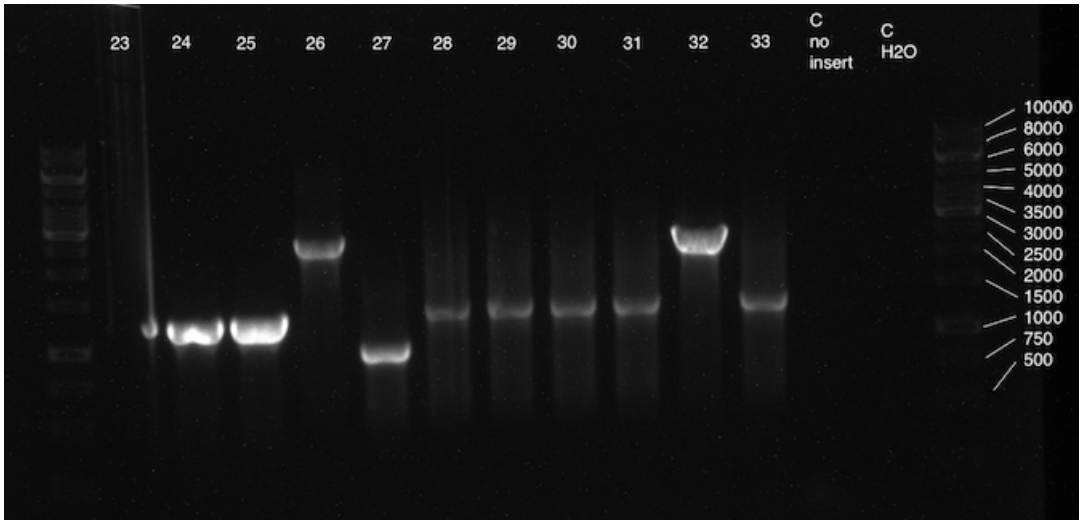

Figure A.9: The image shows the agarose gel of the screening of the CRISPR array products that were amplified using Taq PCR. The CRISPR sequence was screened with primers SK1986 and SK1927. Product number 30 shows a band around the expected size of 1388 bp and was defined as the final construct. The negative controls contained the pWEB-TNC::tracr-pJ23101-cas9deg plasmid as well as no template and the ladder used was Thermo Scientific™ GeneRuler 1 kb DNA Ladder.

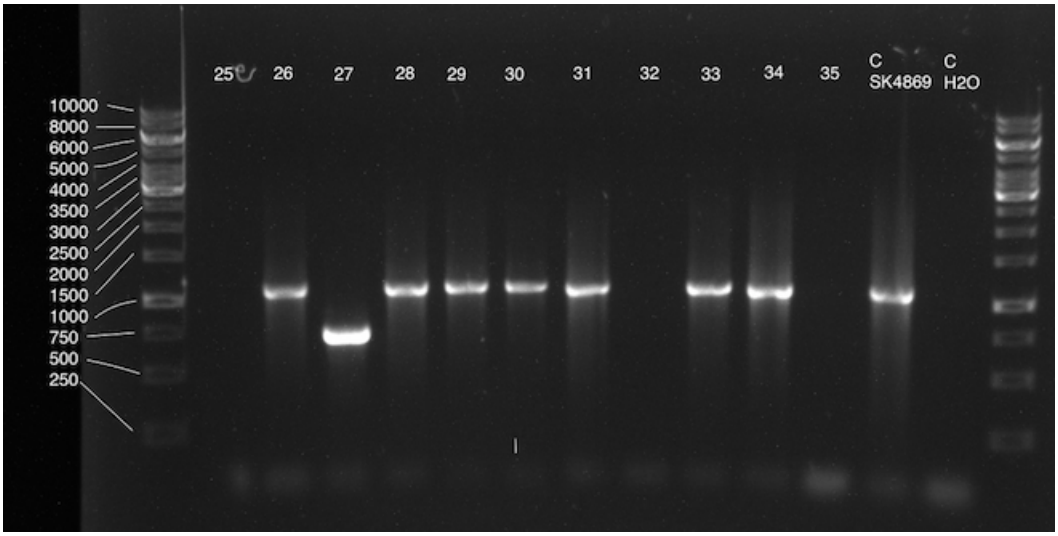

Figure A.10: The image shows the agarose gel of the screening of the CRISPR array products that were amplified using Taq PCR. The CRISPR sequence was screened with primers SK1831 and SK1832. Product number 30 shows a band around the expected size of 1138 bp and was defined as the final construct. The negative controls contained the pWEB-TNC::tracr-pJ23101-cas9deg plasmid as well as no template and the ladder used was Thermo Scientific™ GeneRuler 1 kb DNA Ladder.

A.2 Results

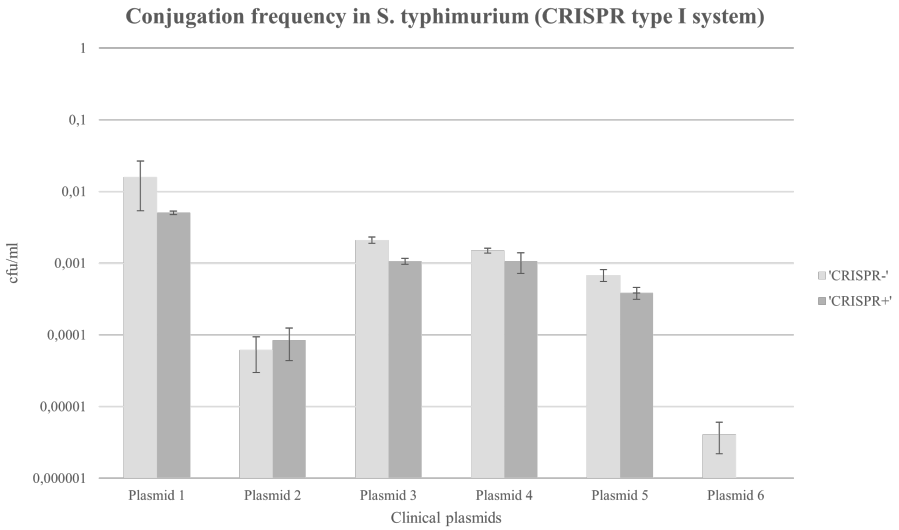

Figure A.11: The diagramme presents the results for the conjugation assays of clinical plasmids into a S. typhimurium with a type I CRISPR system as well as a S. typhimurium that has had the CRISPR system deleted. The CRISPR array contains spacers against the same resistance genes as the constructed CRISPR plasmid in this study. Plasmid number 6 is the pUUH239.2 plasmid.